

June 25, 2022

# Perspectives of measuring gravitational effects of laser light and particle beams

Felix Spengler,<sup>1,\*</sup> Dennis Rätzel,<sup>2,†</sup> and Daniel Braun<sup>1</sup>

<sup>1</sup>*Eberhard-Karls-Universität Tübingen,*

*Institut für Theoretische Physik, 72076 Tübingen, Germany*

<sup>2</sup>*Humboldt Universität zu Berlin, Institut für Physik,*

*Newtonstraße 15, 12489 Berlin, Germany*

## Abstract

We study possibilities of creation and detection of oscillating gravitational fields from lab-scale high energy, relativistic sources. The sources considered are high energy laser beams in an optical cavity and the ultra-relativistic proton bunches circulating in the beam of the Large Hadron Collider (LHC) at CERN. These sources allow for signal frequencies much higher and far narrower in bandwidth than what most celestial sources produce. In addition, by modulating the beams, one can adjust the source frequency over a very broad range, from Hz to GHz. The gravitational field of these sources and responses of a variety of detectors are analyzed. We find that with the planned high-luminosity upgrade of the LHC and an improved design of a recently experimentally demonstrated monolithic pendulum [1], a signal to noise ratio substantially larger than 1 should be achievable. This opens new perspectives of studying general relativistic effects and possibly quantum-gravitational effects with ultra-relativistic, well-controlled terrestrial sources.

## I. INTRODUCTION

With the successful measurement of gravitational waves through LIGO, the measurement of gravitational signals from relativistic sources has gained a lot of interest as it is believed to lead to new insights about gravity, in particular, constraints on modifications of general relativity and potential effects of quantum gravity [2–6]. However, such experiments are limited to detection since the experimenter has no access to the cosmic sources of the signal.

Starting already in the 1970s, proposals were formulated for constructing terrestrial relativistic sources and detectors of their gravitational signals. E.g. in [7–9] a cylindrical micro-wave resonator was proposed as source of a standing gravitational wave and a second concentric cylinder as detector based on photon creation in one of its modes. But it was clear that with the existing technology at the time it was not realistic to create a sufficiently strong source whose radiation could be detected. In recent years there has been renewed interest in the creation and detection of gravitational waves in the lab [10–16].

The gravitational field of electromagnetic radiation has been studied early on [17–19]. It

---

\* Felix-Maximilian.Spengler@Uni-Tuebingen.de

† Dennis.Raetzel@Physik.HU-Berlin.de

gives rise to a range of interesting effects, from an attraction that decays with the inverse of the distance instead of the inverse square [17–20] to frame dragging [21, 22] and other gravitomagnetic effects [23–29]. Their detection has been found to be extremely challenging, see e.g. [20, 22, 24–30]. The phenomenology of the gravitational field of relativistically moving matter is similar to that of light. It can be calculated by Lorentz boosting spacetimes of sources at rest. The result approaches the gravitational field of massless particles in the ultra-relativistic limit [19, 27, 28, 31–33].

As technology has substantially progressed since some of the cited works have been published, both on the side of sources in the form of high-power lasers [34–36] and particle accelerators [37, 38], and in the metrology of extremely weak forces [39–44], it is worthwhile to reassess the possibility to detect the gravitational effects of light and of ultra-relativistic particle beams. Indeed, progress in this direction would enable the test of general relativity (GR) in a new, ultra-relativistic regime (in the sense of special relativity), with an energy-momentum tensor as the source term in Einstein’s equations very different from the one that can be achieved with non-relativistic masses and purely Newtonian gravity, namely with a large off-diagonal component in Cartesian coordinates.

In this article we focus on the acceleration of non-relativistic sensor systems due to the gravitational field of light beams and ultra-relativistic particle beams such as the ones produced at the LHC. We add several new aspects that improve the outlook for experimental observation. Most importantly, we consider trapping of laser light in a cavity, through which the circulating power can be drastically enhanced. Secondly, we consider modulation of the gravitational sources with an adjustable frequency in order to match them to the optimal sensitivity of existing detectors. Several approaches are investigated to that end. The simplest one consists in having laser pulses oscillate to and fro in a cavity, such that the length of the cavity determines the oscillation frequency of the gravitational signal. We also examine the possibility of slowly (kHz frequency) modulating the power with which the cavity is pumped using a continuous wave (cw) or pulsed laser. With the pump power, the power circulating in the cavity is modulated, and thus, also the strength of the gravitational field. Thirdly, we extend the analysis to ultra-relativistic particle beams such as available at the LHC. And finally, we examine several possible sensors for their suitability of measuring the created gravitational fields.

Our work is also motivated by current developments towards measuring gravitational

effects of sources in a quantum mechanical superposition as a possible experimental road to understanding quantum gravitational effects [39, 41, 45, 46]. Creating quantum superpositions of sufficiently large masses is challenging, and it is therefore worthwhile to think about other sources that can be superposed quantum mechanically. We discuss perspectives in this direction for the gravitational sources studied in this paper in Sec.IV.

## II. POTENTIAL SOURCES AND THEIR GRAVITATIONAL FIELD

### A. Laser pulses oscillating in a cavity

To create a strong, high frequency gravitational field, a source of high power and intensity is required. Modern femtosecond laser pulses can reach up to a Petawatt in pulse power. One such laser pulse oscillating in a cavity as illustrated in fig. 1 is a source of short bursts of high energy oscillating to and fro at high frequency. Using the energy momentum tensor, the perturbation to the metric and the resulting Riemann curvature tensor can be calculated within the theory of linearized gravity. For a continuous-wave (*cw*)-laser with power  $P$  and circular polarization, the curvature component relevant to a resonator with axis perpendicular to the beam line of the laser is given by (see eqs.(48-50) in [27], and eq.(1) in [28])

$$R_{\tau\xi\tau\xi} = -\frac{\kappa w_B^2 P}{4\pi c} \frac{1}{\tilde{\rho}^4} \left( \xi^2 - \chi^2 - (4|\mu|^2 \xi^2 \rho^2 + \xi^2 - \chi^2) e^{-2|\mu|^2 \tilde{\rho}^2} \right), \quad (1)$$

in reduced coordinates  $(\tau, \xi, \chi, \zeta) = (ct, x, y, z)/w_B$ , where  $w_B$  is the waist of the laser beam,  $\kappa = 16\pi G/c^4$ ,  $\mu = 1/(1 + i\theta\zeta)$ ,  $\theta$  the opening angle of the laser beam,  $G$  the gravitational constant,  $c$  the speed of light in vacuum, and  $\tilde{\rho} = \sqrt{\xi^2 + \chi^2}$  the dimensional distance of the beam line. The beam propagates in  $z$ -direction. Taking for simplicity  $\theta = 0$  and  $\chi = 0$  (i.e. the observer in the  $x$ - $z$ -plane), neglecting the exponentially decaying term, and switching back to dimensionfull coordinates, we arrive at

$$R_{0x0x} = R_{\tau\xi\tau\xi}/w_B^4 \simeq -4GP/(c^5 \rho^2) \quad (2)$$

with  $\rho^2 = x^2 + y^2 = x^2$  and  $x_0 = ct$ .

Laser *pulses* were considered earlier in [20] in the approximation of an infinitely thin light pencil of length  $L$ . A further exploration in appendix A for the simplified case of box shaped pulses oscillating to-and-fro corroborates the result that close to the beam ( $\rho \ll |z|, |z - D|$ ,

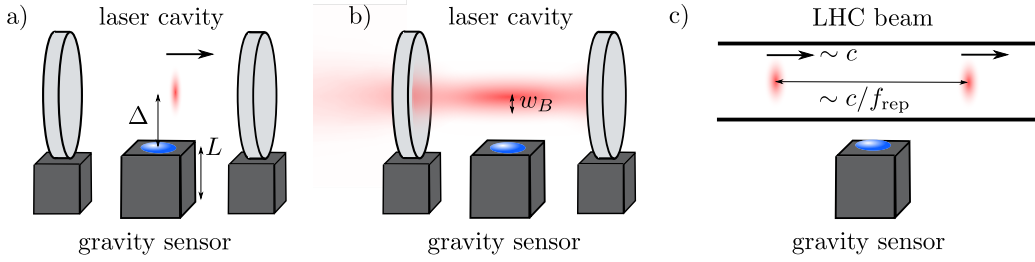


Figure 1. a) Laser pulse oscillating to-and-fro in a cavity. b) cw laser focused to a narrow waist inside a cavity. Its intensity is modulated to create a gravitational field oscillating at kHz frequency. c) Ultrarelativistic particle bunches in an accelerator ring such as the LHC create a very similar gravitational field. In the vicinity of the waist of the laser beam or close to the beamline, a detector picks up resonant mechanical deformations due to the oscillating gravitational forces.

where  $z = 0$  and  $z = D$  are the positions of the two mirrors) (2) gives the correct result, limited, however, to a finite duration of the order of the length of the pulse (see Fig. 8 in [20]) but on the other hand with the cw-power  $P$  replaced by the pulse power  $P_p$  (see eq.(A23)).

The curvature results in a tidal force between two infinitesimally separated points next to the beamline. However, there is no gravitational wave generated as this type of source is not quadrupolar in nature. Rather one can detect the gravitational near-field.

The average power at a given cross section of the beam inside the cavity is  $\bar{P}_{\text{cav}} = N_p \frac{2\tau_p}{\tau_{\text{rt}}} P_p$ , where  $N_p$  is the number of pulses oscillating in the cavity,  $\tau_p$  is the length of the pulse, and  $\tau_{\text{rt}} = \frac{2L_{\text{cav}}}{c}$  is the round trip time in the cavity. As the power enters linearly into the gravitational potential, acceleration, and curvature, all gravitational effects will be proportional to the average power in the cavity.

### 1. Short pulses

A pump laser emitting very short pulses has a broad spectrum in the frequency domain. Coupling these pulses into a cavity of high finesse  $F \approx \frac{\pi(R_1 R_2)^{\frac{1}{4}}}{1 - \sqrt{R_1 R_2}}$  [47] leads to an electric field strength inside the cavity

$$\tilde{E}_{\text{cav}}(\omega) = \tilde{G}_{\text{cav}}(\omega) \tilde{E}_p(\omega), \quad \text{where} \quad \tilde{G}_{\text{cav}}(\omega) = \frac{\sqrt{T_1}}{1 - \sqrt{R_1 R_2} \exp(-i\omega\tau_{\text{rt}})} \quad (3)$$

is the field transfer function, with the intensity transmissivity  $T_1$  of the mirror struck by the pump beam, and the intensity reflectivities of the two mirrors  $R_{1/2}$ , where  $T_1 = 1 - R_1$ . An explicit calculation for the case of rectangular pulses can be found in appendix B, which is based on [48]. If the pulses are very short  $\tau_p \ll \tau_{rt}$  and far apart  $1/f_{rep} \gg \tau_L$ , where  $\tau_L \approx \frac{2F}{\pi}\tau_{rt}$  is the  $1/e$  energy decay time and  $f_{rep}$  is the repetition rate of the pump laser, the pulse enters the cavity at an intensity  $T_1 I_p$ , where the circulating power is enhanced by a factor  $\frac{2F}{\pi}$ , independent of the cavity length. Without any further modification the factors  $T_1$  and  $\frac{2F}{\pi}$  at best cancel up to a factor of 4 (assuming  $R_1, R_2 \simeq 1$ ), leaving little to be gained (see App.B, eq. (B8)). The ways one could imagine improving upon this all involve changes to the mirror that couples the pump laser pulses to the cavity:

- An input coupler is a mirror which is significantly less reflective than what could be achieved with the best available mirrors. It increases the power deposited into the cavity, yet also reduces the cavity finesse. For example, in [49] input couplers are employed to realize enhancement cavities with kilowatt-average-power femtosecond pulses, increasing the average power circulating in the cavity to 670 kW,  $10^3$  times the 420 W average power of the pump laser. Using larger laser spots on the mirrors of the cavity should allow for even stronger pump lasers to be used. With stronger pump lasers, such as the BAT laser in [50] with  $P_{pump} = 300$  kW, an average power within the cavity in the 100 MW range seems plausible.
- A switchable mirror would allow for the full pump beam power to enter the cavity, which means the average cavity power is expected to be the pump laser power enhanced by a factor  $\frac{2F}{\pi}$ . Depending on the cavity's length and the pump laser's repetition rate, the mirror has to be moved on a timescale of  $10^{-9}$  s to  $10^{-3}$  s, the slower end of which seems realistic. A mirror mounted on some mechanics might reduce the precision of its positioning and hence the cavity's finesse. Nonetheless, with a high finesse cavity ( $\frac{2F}{\pi} \sim 10^5$ ) and high-average-power pump lasers ( $P_{pump} \approx 300$  kW [50] ) an average power  $> 20$  GW in the cavity would be achievable.

One limitation when scaling to higher powers is damage to the mirrors. In [51] the cw intensity threshold was determined to be at around  $100$  MW/cm $^2$  before thermal damage sets in. For sub-picosecond pulses the intensity threshold can be exceeded by at least an order of magnitude, as it is done in [49], as long as the average intensity on the mirrors does

not exceed the thermal threshold. For 20 GW (100 MW) cavity power this needs a spot diameter on the mirrors of at least 16 cm (1.1 cm). For the input coupler the limitations are even stricter than for the end mirror as the power passes through the input coupler and creates more heating than when reflected at the surface of the reflecting mirror [49]. Large spot sizes require long cavities, as otherwise the mode in the cavity has a large opening angle and prevents positioning the sensor very close to the beam. For the cited spot-sizes of order 1-10 cm, a cavity length  $L_{\text{cav}} \gtrsim 1$  m suffices. In this work, the increase in power is accounted for by increasing the pulse duration by defining an effective pulse length

$$T_p^{\text{cav}} = T_p^{\text{pump}} f_{\text{rep}} \tau_{\text{rt}} \frac{2F}{\pi} = T_p^{\text{pump}} f_{\text{rep}} \tau_L. \quad (4)$$

For the BAT laser from [50], the repetition rate is  $f_{\text{rep}} = 10$  kHz and the pulse duration of the pump laser is  $T_p^{\text{pump}} = 100$  fs. We further assume  $F = 10^5$  and the signal to be at resonance with the sensor frequency  $\tau_{\text{rt}} = 2\frac{2\pi}{\omega_0}$ , see e.g. Table I. This is consistent with the image of creating a “train” of pulses (one could also imagine pulse stacking, i.e. increasing the pulse power instead). Laser pulses with far higher pulse powers exist. The National Ignition Facility achieves  $5 \cdot 10^{12}$  W peak power [35] but is not as suitable for our purposes due to its low repetition rates. Peak powers of up to  $10 \cdot 10^{15}$  W at repetition rates of up to 10 Hz exist [36] and others with peak powers on the order of  $100 \cdot 10^{15}$  W are planned [52], but will need to achieve high enough average intensities and repetition rates in order to lead to measurable gravitational effects.

## 2. Modulated cw-pumping

Instead of creating a periodic signal by having laser pulses oscillate in a cavity, one could also consider using a cw laser. To create a periodic signal, one can pump the cavity for part of the period and allow for the intensity inside the cavity to decay before switching the pump beam back on for the next period, thus creating a modulated signal with modulation period  $\tau_{\text{mod}}$ . Depending on  $\tau_L$ , the energy within the cavity as a function of time looks more like a periodic sequence of rectangular pulses — in the case of  $\tau_L \ll \tau_{\text{mod}}$  — or like a series of shark fins for  $\tau_L \sim \tau_{\text{mod}}$  (see appendix B).

Using a cw pump laser, the coupling to the cavity is no longer detrimental as for  $\Delta\omega_{\text{FWHM}} \sim 1/\tau_L > \Delta\omega_{\text{pump}}$ , where  $\Delta\omega_{\text{pump}}$  is the line width of the pump beam, the pump

beam couples almost fully to the cavity. The Newtonian gravitational potential for a thin light pencil in the form of a standing wave in the cavity is [17]  $\Phi = \frac{4GP(t)}{c^3} \ln \rho$ , where  $\rho$  is the distance from the beam line and  $P(t)$  is the power passing through the cross section with the detector, i.e.  $P(t) = \bar{P}_{\text{cav}}(t)$  in this case. For the slowly moving detectors envisaged here (speeds  $v \ll c$ ), all equations of motion are the same for the source consisting of the standing wave or the propagating one.

For long modulation periods  $\tau_{\text{mod}} \gg \tau_L$ , the maximum power in the cavity is  $P_{\text{cav}}^{\text{max}} = \frac{2F}{\pi} P_{\text{pump}}$ , for approximately half the modulation period. Commercially available cw laser systems reach continuous powers of 500 kW in multimode operation and up to 100 kW in single-mode operation (see e.g. [53]). Combining this with a high finesse cavity  $F \sim 10^6$  leads to an average power in the cavity of

$$\bar{P}_{\text{cav}} = \frac{1}{2} \frac{2F}{\pi} P_{\text{pump}} \sim 100 \text{ GW}. \quad (5)$$

Shorter cavities lead to lower  $\tau_L$  at the same finesse and without decreasing the average power. The same considerations for the spot size and length of cavity as mentioned for the laser pulses apply also in the cw case for positioning the detector sufficiently close to the beam waist and neglecting higher order effects in the opening angle [27]. For a 1 m-long high-finesse cavity ( $F \sim 10^6$ ) the decay time  $\tau_L$  is in the low millisecond range, which is too slow for some of the proposed detector setups. This could be circumvented by implementing techniques such as Q-switching, with which the decay of energy within the cavity can be accelerated, and the aforementioned switchable mirrors. Also, the energy buildup can be modulated to a certain degree by pumping. For short modulation periods,  $\tau_{\text{mod}} \approx \tau_L$ , the cavity is never fully pumped. The average power in the cavity can at most be a fraction  $< (1 - e^{-\tau_{\text{mod}}/(2\tau_L)})$  of the maximum power  $\frac{2F}{\pi} P_{\text{pump}}$ . For  $\tau_{\text{mod}} \gtrsim \tau_L$  it is barely possible to achieve a large relative modulation amplitude of the intensity due to incomplete decay during the second half period of the modulation cycle. Here the aforementioned techniques to quickly dump energy from the cavity are required.

## B. The Large Hadron Collider (LHC)

Instead of high-energy-laser pulses, one can also investigate the use of ultra relativistic particle beams consisting of high-energy bunches as a source, such as the one at LHC. A

particle beam in the relativistic limit is, from a gravitational perspective, the same as a laser beam: the rest mass of the protons  $m \simeq 938 \text{ MeV}/c^2$  makes a negligible contribution to their energy for achievable particle energies of about 6.5 TeV and both charge and spin are irrelevant [31–33]. To very good approximation, the energy-momentum relationship is then  $E = cp$  where  $p$  is the momentum of the protons, just as for photons. In the ring of the LHC there are 2808 bunches of protons at maximum capacity, each bunch with a total energy of  $\sim 10^5 \text{ J}$ . One bunch is approximately 30 cm long, contains  $1.15 \cdot 10^{11}$  protons, and can be squeezed down to a transverse diameter of  $\sim 16 \mu\text{m}$  (see [37]). To excite a resonator at its eigenfrequency  $\nu_0 = \omega_0/(2\pi)$ , the bunches have to pass by the detector with rate  $\nu_0$ , or the beam must be modulated with frequency  $\nu_0$ . The 2808 bunches spread over a ring of 26,659 m length moving at speed close to  $c$  entail a rate of 31.2 MHz. A single bunch going around the ring passes with a frequency of 11 kHz. To achieve lower frequencies one could, for example, periodically modulate the beam position. This would result in a scheme similar to that of the cw laser cavity, where the LHC beam is active for half the sensors oscillation period  $\tau_p = \frac{1}{2} \frac{2\pi}{\omega_0}$  with an effective pulse power  $P_p = P_{\text{avg}}^{\text{LHC}}$ , where  $P_{\text{avg}}^{\text{LHC}}$  is the nominal average power of the LHC. The pulse power of the LHC beam is orders of magnitude smaller than that of extreme-power-laser pulses, but the proton bunches are much longer ( $\sim 1 \text{ ns}$ ) than the laser pulses. This results in a higher average power of  $P_{\text{avg}}^{\text{LHC}} \approx 3.8 \cdot 10^{12} \text{ W}$ , which is orders of magnitude larger than the average power of laser pulses oscillating in a cavity and about 40 times the average power that can be contained in a cavity pumped by the cw laser considered above (see table I). Therefore, from the perspective of the strength of the gravitational source, the LHC beam might be preferable. A potential drawback compared to the laser-based sources is the lack of flexibility in frequency. This can be compensated, however, by considering detectors with tunable resonance frequency. Besides protons, it is also possible to use heavy nuclei, or partially ionized heavy atoms. The latter have the advantage that the corresponding beams can be laser-cooled (see the discussion in Sec.IV B). Upgrades of the LHC to use heavy ions are currently considered [54], and also under development at Brookhaven National Lab [55].

|                    | pulses in cavity  | cw cavity              | LHC                   |
|--------------------|---|------------------------|-----------------------|
| $P_p$              | $3 \cdot 10^{14}$ W   | $2 \cdot 10^{11}$ W    | $10^{14}$ W           |
| $T_p^{\text{cav}}$ | $100 \text{ fs} \cdot 10 \text{ kHz} \frac{8 \cdot 10^5}{\omega_0}$ † | $\frac{\pi}{\omega_0}$ | $10^{-9} \text{ s}$ * |
| $P_{\text{avg}}$   | $2 \cdot 10^{10}$ W   | $1 \cdot 10^{11}$ W    | $3.8 \cdot 10^{12}$ W |
| $w_B$              | $< 100 \mu\text{m}$   | $< 100 \mu\text{m}$    | $16 \mu\text{m}$      |

Table I. Comparison of relevant numbers of the LHC beam and the laser-based sources from II A 1 and II A 2:  $P_p$  pulse power,  $P_{\text{avg}}$  power averaged over time,  $w_B$  waist of beam.  $\omega_0$  is the desired signal frequency, assumed in Sec.III to be one of the resonances frequencies of the detector.

† A switchable mirror is assumed for the pulses in the cavity. The pulses are assumed to be effectively stacked together to a larger circulating pulse, see eq.(4).

\* The effective pulse length  $T_p^{\text{cav}}$  for the LHC corresponds to a single proton bunch, but a much slower modulation of the beam in resonance with  $\omega_0$  can be envisaged.

### III. DETECTORS

We consider three types of detectors, a mechanical rod, a detector based on superfluid helium-4 coupled parametrically to a superconducting microwave cavity, and a monolithic pendulum. The latter two are optomechanical detectors close to the quantum limit. Quantum optomechanical detectors have been studied in great detail and different configurations over recent years, both theoretically and experimentally [56–59]. They have been considered for high precision sensing [60] in particular, force sensing [61] and theoretical work has been performed to derive general limits for sensing of oscillating gravitational fields with such systems [62, 63].

#### A. Mechanical response of a rod

A spatially dependent gravitational acceleration compresses a 1D deformable resonator according to its Young modulus  $Y$ . In the plane orthogonal to a pulsed energy beam, the gravitational acceleration acting upon a non relativistic object is equivalent in the near field to the force resulting from a pulsed Newtonian potential  $\Phi = \frac{4GP(t)}{c^3} \ln \rho$ , where  $\rho$  is the distance from the beam line and  $P(t)$  is the power passing through the cross section with the

detector (see appendix A for a detailed derivation). The wave equation for the displacement field  $u(x, t)$ , describing the relative position of an element of the rod from its equilibrium location  $x$  is given in [64, p.416],

$$\varrho_m \partial_t^2 u(x, t) - Y \partial_x^2 u(x, t) = -\varrho_m \partial_x \Phi(x, t), \quad (6)$$

where the resonator is extended in the  $x$  direction, orthogonal to the beam, and  $\varrho_m$  is its mass density. The length contraction due to modification of space-time is negligible in comparison to the elastic effect considered here, as it comes with an additional factor  $c_s^2/c^2$  [65], where  $c_s = \sqrt{Y/\varrho_m}$  is the speed of sound in the rods material.

The displacement field can be expanded into the spatial eigenmodes

$$w_n(x) = \cos \left( \left( n + \frac{1}{2} \right) \frac{\pi}{L} (x - \Delta) \right)$$

of the free equation complying with the boundary conditions, i.e. the tip of the resonator distant from the source was chosen to be fixed in place by the support (hence  $w_n(L + \Delta)$  has to vanish and  $\partial_x w_n|_{x=\Delta}$  has to vanish at the other tip), where  $n \in \mathbb{N}_0$ ,  $\Delta$  is the distance of the tip of the rod from the source, and  $L$  is the length of the resonator. The spatial eigenmodes are orthonormal with respect to the scalar product  $\langle a|b \rangle = (2/L) \int_{\Delta}^{\Delta+L} a(x)b(x) dx$ . The total displacement field is then given by  $u(x, t) = \sum_{n=0}^{\infty} \xi_n(t) w_n(x)$ . The differential equation for the temporal amplitude  $\xi_n(t)$  resulting from the projection of (6) onto the  $n$ th spatial eigenmode is then given by

$$\ddot{\xi}_n(t) + \frac{\omega_n}{Q} \dot{\xi}_n(t) + \omega_n^2 \xi_n(t) = -\frac{2}{L} \int_{\Delta}^{L+\Delta} dx w_n(x) \partial_x \Phi(x, t), \quad (7)$$

where  $\omega_n = c_s \left( n + \frac{1}{2} \right) \frac{\pi}{L}$  is the frequency of the mode and a linear dissipation term  $\gamma_n \partial_t u(x, t)$  with rate  $\gamma_n = \varrho_m \frac{\omega_n}{Q}$  was added to equation (6) in order to include dissipation from the elastic modes of the resonator.

In the case of resonant excitation, the amplitude of the steady state solution in the lowest eigenmode  $\xi_0(t) = A(\omega_0) \sin(\omega_0 t)$ , reached after a transient time  $\frac{Q}{\omega_0}$  is then given by

$$A(\omega_0) = \frac{Q}{\omega_0^2} \int_0^{2\pi/\omega_0} dt \frac{\omega_0}{\pi} \cos(\omega_0 t) \int_{\Delta}^{L+\Delta} dx \frac{2}{L} \cos \left( \frac{\pi}{2L} (x - \Delta) \right) (-\partial_x \Phi(x, t)), \quad (8)$$

where the integration of  $t$  over one mechanical period gives the Fourier component of the driving force corresponding to this mechanical mode. At this point we assumed the pulse to be centered around  $t = 0$  and to be repeating at intervals of  $\frac{2\pi}{\omega_0}$ .

With the periodic Newtonian potential from appendix A

$$\Phi(x, t) = \frac{4GP_p}{c^3} \ln(x) \llcorner_{\Sigma}(t) \quad (9)$$

$$\implies -\partial_x \Phi(x, t) = -\frac{4GP_p}{c^3} \frac{1}{x} \llcorner_{\Sigma}(t), \quad (10)$$

where  $P_p$  is the pulse power and  $\llcorner_{\Sigma}(t) = \sum_n \left[ \Theta\left(t - \frac{n2\pi}{\omega_0} - \frac{\tau_p}{2}\right) - \Theta\left(t - \frac{n2\pi}{\omega_0} + \frac{\tau_p}{2}\right) \right]$  is a sum of rectangular pulses of duration  $\tau_p$ . The integral over the oscillation period in eq.(8) returns

$$\int_0^{2\pi/\omega_0} dt \frac{\omega_0}{\pi} \cos(\omega_0 t) \llcorner_{\Sigma}(t) = \frac{2}{\pi} \sin \frac{\omega_0 \tau_p}{2} \approx \begin{cases} \frac{\omega_0 \tau_p}{\pi} & \text{for } \tau_p \omega_0 \ll 2 \\ \frac{2}{\pi} & \text{for } \tau_p \approx \frac{\pi}{\omega_0} \end{cases}. \quad (11)$$

In the extreme cases this is equivalent to the substitution  $P_p \frac{2}{\pi} \sin \frac{\omega_0 \tau_p}{2} \approx P_p \frac{\tau_p \omega_0}{\pi} = 2P_{\text{avg}}$  (for  $\tau_p \ll \frac{2}{\omega_0}$ ) and  $P_p \frac{2}{\pi} \sin \frac{\omega_0 \tau_p}{2} \approx \frac{4}{\pi} P_{\text{avg}}$  (for  $\tau_p \approx \frac{\pi}{\omega_0}$ ) in eq.(8), where  $P_{\text{avg}} \equiv \frac{\text{energy in the cavity}}{\text{oscillation period}} = \frac{P_p \tau_p}{\frac{2\pi}{\omega_0}}$  is the power in the cavity averaged over one mechanical period. The spatial integration scales as

$$\int_{\Delta}^{L+\Delta} dx \frac{2}{L} \cos\left(\frac{\pi}{2L}(x - \Delta)\right) \frac{1}{x} \propto \begin{cases} \frac{4}{\pi \Delta} & \text{for } L \ll \Delta \\ \frac{2 \ln \frac{L}{\Delta}}{L} & \text{for } L \gg \Delta \end{cases}. \quad (12)$$

With this, a resonant maximum amplitude of

$$A(\omega_0) = \frac{4GP_p Q}{\omega_0^2 c^3} \frac{2}{\pi} \sin\left(\frac{\omega_0 \tau_p}{2}\right) \int_{\Delta}^{L+\Delta} dx \frac{2}{L} \cos\left(\frac{\pi}{2L}(x - \Delta)\right) \frac{1}{x} \quad (13)$$

$$\approx \frac{32GP_{\text{avg}} Q}{\pi \omega_0 c^3} \begin{cases} \begin{cases} \frac{1}{\omega_0 \Delta} & \text{for } \tau_p \omega_0 \ll 2 \\ \frac{2}{\pi \omega_0 \Delta} & \text{for } \tau_p = \frac{\pi}{\omega_0} \end{cases} & \text{and } L \ll \Delta \\ \begin{cases} \frac{1}{c_s} \ln \frac{L}{\Delta} & \text{for } \tau_p \omega_0 \ll 2 \\ \frac{2}{\pi c_s} \ln \frac{L}{\Delta} & \text{for } \tau_p = \frac{\pi}{\omega_0} \end{cases} & \text{and } L \gg \Delta \end{cases} \quad (14)$$

is reached in the steady state of prolonged driving.

Even though it might seem favorable to increase  $L$  because of the logarithmic scaling in eq. (12), the inhomogeneous driving force leads to excitations of multiple mechanical modes which, for a non perfectly rigid support, can couple. Also, the distance between the detector and the beam has to be much smaller than the length of the source cavity (or radius of the ring resonator) for the contributions of the recoil of the mirrors (or deflecting magnetic

fields) to be negligible. These two effects might lead to the break down of the logarithmic scaling before it makes a difference.

As the rod was chosen to be fixed by the support at its tip at the far side of the beam, the lowest eigenmode has wavelength  $\lambda = \frac{2\pi c_s}{\omega_0} = 4L$ . The minimum distance from the beam is  $\Delta \approx w_B$ , where for the purposes of this estimation, we saturate this lower bound on  $\Delta$ . Assuming for orientation numerical values of aluminum,  $c_s = c_s^{\text{Al}} = 6420 \text{ m/s}$ ,  $\omega_0 = 2\pi \cdot 10^9 \text{ Hz}$  and  $Q = 10^6$  for the rod, the laser cavity introduced in II A 1 ( $P_{\text{avg}} = 20 \text{ GW}$ ,  $w_B \approx 100 \mu\text{m}$ ) would result in an amplitude of  $A \approx 10^{-34} \text{ m}$  at the freely oscillating tip. Here, one is in the short rod limit of eq. (12) due to the very high frequencies.

Even for higher quality factors of  $Q = 10^8$ , one ends up at  $A \approx 10^{-32} \text{ m}$ , roughly fourteen orders of magnitude smaller than the amplitude of the oscillations of the arms of LIGO when detecting gravitational waves. On the other hand, the setup proposed here produces mechanical oscillations at up to GHz frequency and on a sub-mm length scale rather than 4 km long arms. The relative change of length,  $A(\omega_0)/L \approx 10^{-26}$  is still about four orders of magnitude away from the corresponding value of LIGO.

At resonance, the noise spectral density at resonance for a resonant-bar type detector is given by

$$S_A^{\text{th}} = \frac{4k_B T Q}{\omega_0^3 M_{\text{eff}}} \implies A_{\text{th}} = \sqrt{\frac{S_A^{\text{th}}}{\tau_{\text{int}}}} \quad (15)$$

according to [64, p.440], where  $M_{\text{eff}} = \int \varrho_m A_R(w_0(x))^2 dx$  is the effective mass of the mode with the rod cross section  $A_R$ , and  $A_{\text{th}}$  is the amplitude resulting from the thermal noise after integration time  $\tau_{\text{int}}$ . At  $\omega_0 = 2\pi \cdot 1 \text{ GHz}$  the thermal sensitivity limit for temperatures below  $T = 48 \text{ mK}$  is already below the standard quantum limit on noise spectral density for a resonant mass detector [66],

$$S_A^{\text{SQL}} = \frac{4\hbar Q}{M_{\text{eff}} \omega_0^2}. \quad (16)$$

At frequencies below the megahertz range, the thermal noise is the limiting factor. For  $Q = 10^6$ ,  $M_{\text{eff}} = \frac{\pi}{8} \varrho_{\text{Al}} L^3$  (assuming a constant aspect ratio) with the mass density of aluminum  $\varrho_{\text{Al}} = 2.7 \text{ g/cm}^3$  and a frequency of  $\omega_0 = 2\pi \cdot 1 \text{ GHz}$  the sensitivity is

$$\sqrt{S_A^{\text{SQL}}} = \sqrt{\frac{4\hbar Q}{M_{\text{eff}} \omega_0^2}} \approx 4 \cdot 10^{-17} \frac{\text{m}}{\sqrt{\text{Hz}}},$$

meaning that for 1 year of integration time at best an amplitude of  $10^{-20} \text{ m}$  can be detected. Nonetheless, even for very short integration times one is already below the minimum error

given by the zero-point fluctuation in this frequency range  $x_{\text{zpf}} = \sqrt{\frac{\hbar}{M_{\text{eff}}\omega_0}} \sim 10^{-14} \text{ m}$ .

For the LHC, where the rate of bunches passing by is  $\nu = 31.2 \text{ MHz}$ , for the purposes of this estimation, we assume that the same amount of protons is split into 88925 bunches instead of 2808 such that we reach the frequency  $\omega_0 = 2\pi \cdot 1 \text{ GHz}$  while keeping the same average power. With pulses filling half a period, the peak power is  $P_p = 2P_{\text{avg}}$ . Using the same  $c_s = 6420 \text{ m/s}$  and  $Q = 10^6$  and the values of the LHC ( $P_{\text{avg}} = 3.8 \cdot 10^{12} \text{ W}$ ,  $w_B = 16 \mu\text{m}$ ) one would expect the amplitude of the resonator to be  $A \approx 9 \cdot 10^{-32} \text{ m}$ , which is at least two orders of magnitude larger than that caused by the oscillating laser pulse from Sec.IIA 1. For higher quality factors  $Q = 10^8$  amplitudes of  $A \approx 9 \cdot 10^{-30} \text{ m}$  might be possible. At far lower frequencies, where the limit  $L \gg \Delta$  becomes relevant in eq.(13), a lower speed of sound, for example  $c_s = 100 \text{ m/s}$ , is also very beneficial and the amplitude now scales as  $1/\omega_0$ , whereas the SQL scales as  $\sqrt{\omega_0}$  (assuming  $M_{\text{eff}} \propto L^3$ ). However, at some point the constant (again, assuming  $M_{\text{eff}} \propto L^3$ , which will be unrealistic for  $L$  beyond the centimeter range) thermal noise far exceeds the quantum noise limit and one quickly ends up with a meter long rod, outside the “close to the beam” limit, whilst still not within range of detection.

To probe the limit  $L \gg \Delta$  we assume  $\omega_0 = 2\pi \cdot 1 \text{ kHz}$ ,  $Q = 10^6$ ,  $c_s = 6420 \text{ m/s}$  implying an extreme  $L \approx 4 \text{ km}$ . Then, the expected amplitude from the laser pulses in sec. II A 1 is  $A \approx 2 \cdot 10^{-25} \text{ m}$ , for the cavity pumped with a modulated cw laser  $A \approx 4 \cdot 10^{-25} \text{ m}$ , while we expect an amplitude of  $A \approx 8 \cdot 10^{-24} \text{ m}$  for the LHC beam (which would have to be modulated to reach such low frequencies). Assuming a temperature of  $T = 5 \text{ mK}$  the sensitivity is

$$\sqrt{S_A^{\text{th}}} = \sqrt{\frac{4k_B T Q}{\omega_0^3 M_{\text{eff}}}} \approx 10^{-17} \frac{\text{m}}{\sqrt{\text{Hz}}}, \quad (17)$$

leaving the amplitudes still unmeasurable even for unreasonably long integration and rise times and an unreasonable rod length. Increasing the quality factor to  $Q = 10^8$  is not enough to overcome this.

## B. Superfluid Helium detector

In [67] Singh et al. study the acoustic motion of superfluid helium-4 coupled parametrically to a superconducting microwave cavity as a detection scheme for continuous-wave

gravitational signals. With few theoretical adaptations the system can be adapted to the near field-case considered here. The very high Q-factors and sensitive microwave transducer means this is essentially a better version of the deformable rod considered in section III A.

We assume the source to be aligned along the  $z$  axis orthogonal to a cylindrical superfluid helium detector with its axis of symmetry along the  $x$  axis ( $y = 0$ ). The equation of motion for the  $x$  component of the displacement field  $\mathbf{u}$  (of the fluid helium inside the chamber) is given by

$$\partial_t^2 u^i - \frac{S}{\varrho_m} \nabla^2 u^i - \frac{K + \frac{1}{3}S}{\varrho_m} \partial^i (\nabla \cdot \mathbf{u}) = -\delta_{ix} \varrho_m \partial_x \Phi(x, t), \quad (18)$$

where  $K$  is the bulk modulus,  $S$  is the shear modulus (which are used instead of the Lamé coefficients for better readability), and  $\Phi(x, t)$  the gravitational potential. Eq. (18) is the three-dimensional version of eq. (6). As before, the displacement field can be linearly decomposed into its spatial eigenmodes

$$\mathbf{w}_{lmn}(\mathbf{x}) = \frac{1}{N} \nabla \left( J_m(k_m(l) \varrho_x) \cos(m\varphi_x) \cos\left(\frac{n\pi}{L} \left(x - x_0 + \frac{L}{2}\right)\right) \right), \quad (19)$$

where  $\varrho_x$  is the distance from the  $x$  axis,  $k_m(l)$  is a wavevector that is related to the  $l$ th root of the  $m$ th Bessel function,  $\varphi_x$  is the polar angle in the plane orthogonal to the  $x$  axis,  $N$  is the normalization such that  $\max_{\mathbf{x}} |\mathbf{w}_{lmn}| = 1$ ,  $L$  is the length of the helium chamber, and  $x_0$  is its center point.

For our purposes, we reduce this to the one dimensional problem from section III A. Here, the boundary conditions are different from the rod in III A, as the displacements at both ends of the cylinder have to vanish. Therefore the ground mode ( $n = 1, l = 0, m = 0$ ) is now given by  $w_x = \sin\left(\frac{\pi}{L}(x - \Delta)\right)$ .

Following Singh et al. [67], the position noise spectral density of the temporal displacement field amplitude  $\xi$  caused by Brownian motion on resonance is given by

$$S_{\xi\xi}^{\text{th}} = \frac{4k_B T Q_{\text{He}}}{M_{\text{eff}} \omega_0^3}, \quad (20)$$

where  $M_{\text{eff}} = \int \varrho_m |\mathbf{w}|^2 dV$ , integrated over the whole detector, is the effective mass of the eigenmode. This is the same as eq. (15), but a factor of 2 had to be added compared to the form in [67] to obtain the single sided density ( $\omega_0 > 0$ ) as is used in [64]. With the susceptibility on resonance  $\chi = \frac{Q_{\text{He}}}{iM_{\text{eff}}\omega_0^2}$ , this results in a thermal force noise spectral density

(on resonance) of

$$S_{FF}^{\text{th}} = |\chi|^{-2} S_{\xi\xi}^{\text{th}} = 4k_B T M_{\text{eff}} \frac{\omega_0}{Q_{\text{He}}}. \quad (21)$$

We further follow [67], where the force sensitivity  $\sqrt{S_{FF}^{\text{th}}}$  of the detector results in the lower bound to the detectable force over an integration time  $\tau_{\text{int}}$  with  $2\sigma$  uncertainty given by

$$\bar{F}_{\text{min}} \approx 2 \sqrt{\frac{S_{FF}^{\text{th}}}{\tau_{\text{int}}}} = \sqrt{\frac{16k_B T M_{\text{eff}} \omega_0}{\tau_{\text{int}} Q_{\text{He}}}}. \quad (22)$$

The Fourier component of the force corresponding to the considered lowest-frequency mode is given by

$$\bar{F}_{\text{eff}} = \frac{16GM_{\text{eff}}P_{\text{p}}}{\pi L c^3} \sin\left(\frac{\omega_0 \tau_{\text{p}}}{2}\right) \int_{\Delta}^{\Delta+L} \frac{\sin\left(\frac{\pi(x-\Delta)}{L}\right)}{x} dx, \quad (23)$$

where the temporal Fourier component from eq.(11) reappears. This integral converges to  $\approx 1.85$  for  $L \gg \Delta$ . Assuming once again a constant aspect ratio, i.e.  $M_{\text{eff}} \sim L^3$  (which does not necessarily have to be the case), this leads to a scaling of

$$\bar{F}_{\text{min}} \sim L \quad \text{and} \quad \bar{F}_{\text{eff}} \sim L^2,$$

implying that for large enough  $L$  the force should be detectable although limitations apply, as discussed in section III A. Interestingly, the difference in boundary conditions, as compared to section III A, leads to a weaker scaling for  $L \gg \Delta$ , as the logarithmic dependence stems from the overlap of the mode function with the steep end of the  $\frac{1}{x}$  driving force, whereas the modes of the helium have to vanish at the end of the container. Nevertheless, the additional logarithmic factor is basically irrelevant on realistic length scales.

To get a feeling for the orders of magnitude, we start off with the numbers from the actual experimental setup from Singh et al. [67]. We set  $\tau_{\text{int}} = 250$  d,  $Q_{\text{He}} = 6 \cdot 10^{10}$ ,  $L = 4$  cm,  $r = 1.8$  cm (radius),  $c_s = 220$  m/s, and  $\varrho_{\text{He}} = 145$  kg/m<sup>3</sup>. This implies  $\omega_0 = 2\pi \cdot 2.8$  kHz,  $M_{\text{eff}} = 3$  g,  $T = 5$  mK. This results in a minimum detectable force  $\bar{F}_{\text{min}} \approx 4 \cdot 10^{-21}$  N. Choosing the LHC as a source, we assume  $\Delta = w_B$  and set the average power to  $P_{\text{p}} = P_{\text{avg}}^{\text{LHC}} = 3.8 \cdot 10^{12}$  W,  $\tau_{\text{p}} = \frac{1}{2} \frac{2\pi}{\omega_0}$ , resulting in  $\bar{F}_{\text{eff}} \approx 6.6 \cdot 10^{-24}$  N. Going further from the beamline (by less than  $L$ ) to account for shielding and the Helium container only decreases the effective force slightly (for  $\Delta = 16$   $\mu$ m  $\rightarrow \Delta = 3$  cm,  $F_{\text{eff}}$  decreases by a factor of 4) as there is limited contribution from the liquid Helium at the ends of the container to the ground mode.

Hence, at full amplitude and one week of integration time, the 4 cm prototype detector is lacking about 3.5 of magnitude in sensitivity. Under otherwise identical assumptions, the proposed first generation (0.5 m) detector will be about 2.5 orders of magnitude from being sensitive enough to detect the gravitational signal from the LHC.

### C. High-Q milligram-scale monolithic pendulum - applied to pulsed-beam gravity sources

In a recent publication, Matsumoto et al. described the manufacturing of a pendulum and presented its properties [68]. They found it to have a very high quality factor for a small scale system and even higher when combined with an optical spring. Different from the extended oscillators considered in the earlier subsections, the pendulum does not rely on the projection of the gravitational acceleration on an elastic mode but rather on the gravitational force on the pendulum mass relative to the support. A mechanical oscillator has to be of small scale to be close enough to the source for the gravitational acceleration to be significant, while the gravitational effects on the pivot point need to remain negligible.

For the  $l = 1$  cm,  $m = 7$  mg pendulum a mechanical Q-factor of  $Q_m = 10^5$  was measured in [68] at  $\omega_m = 2\pi \cdot 4.4$  Hz. Introducing an optical spring to modulate the frequency, the effective Q-factor is expected to scale as  $Q_{\text{eff}} \approx Q_m \left( \frac{\omega_0}{\omega_m} \right)^2$  (the effective frequency of the coupled system was renamed from  $\omega_0$  ( $Q_0$ ) in the original work [68] to  $\omega_m$  ( $Q_m$ ) for consistency). At  $\omega_0 = 2\pi \cdot 280$  Hz a sensitivity of  $3 \cdot 10^{-14} \frac{\text{m}}{\sqrt{\text{Hz}}}$  was demonstrated with a reduced  $Q$ -factor of 250, with thermal motion the main source of noise. According to eq. (15) this corresponds to a temperature of a few Millikelvin. As the effective temperature scales as [68]

$$T_{\text{eff}} = \frac{4T}{Q_m(\omega_0/\omega_m)^2}, \quad (24)$$

Matsumoto et al. expect to be able to reach an effective temperature of a few  $\mu\text{K}$ . In an update to this [1] Cataño-Lopez et al. described an improved version of this pendulum, with a measured mechanical Q-factor of  $Q_m = 2 \cdot 10^6$  at a frequency of  $\omega_m = 2\pi \cdot 2.2$  Hz, which with the optical spring is tunable in the frequency range of  $400 \text{ Hz} < \frac{\omega_0}{2\pi} < 1800 \text{ Hz}$ . Due to the increased frequency, and the scaling of  $T_{\text{eff}}$ , thermal noise  $\sqrt{S_{\text{th}}} = \sqrt{\frac{4k_B Q_{\text{eff}} T_{\text{eff}}}{M_{\text{eff}} \omega_0^3}}$  becomes less relevant at higher frequencies and quantum noise given by eq. (16) [66] is now the dominant source of noise.

For a pulsed-beam source, the gravitational acceleration in radial direction for the duration of a pulse is given by

$$a_{\text{grav}}^p = -\frac{4GP_p}{c^3} \frac{1}{\rho}, \quad (25)$$

where  $G$  is the Newton gravitational constant,  $P_p$  is the pulse power, and  $\rho$  is the distance from the beam. For this setup  $\rho$  is limited by the radius of the pendulum mass (1.5 mm) and the beam width ( $\ll$  .5 mm), so  $\rho = 2$  mm is a reasonable estimate.

The displacement resulting from prolonged ( $\tau \sim \frac{2\pi Q_{\text{eff}}}{\omega_0}$ ) driving on resonance is given by

$$x_{\text{grav}} = \frac{\bar{a}_{\text{grav}}}{\omega_0^2} Q_{\text{eff}} = \frac{\bar{a}_{\text{grav}} Q_m}{\omega_m^2} = \frac{8GP_p \sin\left(\frac{\omega_0 \tau_p}{2}\right) Q_m}{\pi c^3 \omega_m^2} \frac{1}{\rho}, \quad (26)$$

where  $\bar{a}_{\text{grav}}$  is the Fourier component of  $a_{\text{grav}}(t)$  on resonance, and  $\sin\left(\frac{\omega_0 \tau_p}{2}\right)$  results from the overlap of the rectangular pulses with the sinusoidal oscillation calculated in eq.(11). This is very similar to eq. (13) from section III A but with the distance from the source  $\rho$  rather than the length of the resonator. We now consider how the pendulum would react to the different gravitational sources discussed above.

### 1. Cavity pumped with cw laser

Thanks to the fortunate scaling of  $Q_{\text{eff}}$ , larger frequencies are favorable (when not accounting for the increase in rise time) until other detrimental effects such as coupling to higher modes or resonances of the support become relevant. For the middle of the noise window,  $\omega_0 = 2\pi \cdot 1$  kHz and the cw laser cavity from II A 2 with a power in the cavity of  $P_p = 200$  GW for half the oscillation period the expected amplitude resulting from the gravitational signal  $x_{\text{grav}} \approx 6.6 \cdot 10^{-18}$  m is slightly smaller than the zero point fluctuation  $x_{\text{zpf}} = \sqrt{\frac{\hbar}{m\omega_0}} \approx 5 \cdot 10^{-17}$  m but the on-resonance SQL sensitivity [66]  $\sqrt{S_{\text{SQL}}} = 2x_{\text{zpf}} \sqrt{\frac{Q_{\text{eff}}}{\omega_0}} = \sqrt{\frac{4\hbar Q_{\text{eff}}}{m\omega_0^2}} \approx 8 \cdot 10^{-13} \frac{\text{m}}{\sqrt{\text{Hz}}}$  shows that once again unreasonably long integration times of order  $10^{10}$  s would be needed to measure the signal corresponding to the oscillating pendulum position.

The SQL refers to amplitude-and-phase measurements of that position. In principle, due the precisely known frequency, quantum non-demolition measurements allow continuous monitoring of the oscillation [69]. With a “single-transducer, back-action evading measurement”, one can estimate a quadrature of the oscillator with an uncertainty that scales  $\propto (\beta\omega_0\tau_m)^{-1/2}$ , where  $\tau_m$  is the relevant measurement time or inverse filter width, and  $\beta$  a

numerical factor that can reach a value of order one (see eq. 3.21a,b in [69] and eqs.(32,33) in [70]). After upconverting the kHz signal to the GHz regime one can use modern microwave amplifiers with essentially no added noise [71–74]. Upconversion to microwave frequency range was already discussed in the 1980s [70] and can be achieved by having the sensor modulate the resonance frequency of a micro-wave cavity. Additional sensitivity can be gained with a large number  $N$  of sensors arranged along the laser beam or particle beam. Classical averaging their signal leads to a noise reduction of  $1/\sqrt{N}$  in the standard deviation. When several sensors all couple to the same micro-wave cavity, one might even hope to achieve “coherent averaging”, in which case the noise reduction scales as  $1/N$  [75, 76].

With  $N = 1$  and a signal of kHz frequency, the sensitivity of the monolithic pendulum resulting from the standard quantum noise limit  $\sqrt{S_{\text{SQL}} \approx 8 \cdot 10^{-13} \frac{\text{m}}{\sqrt{\text{Hz}}}}$  is 3 orders of magnitude too small to measure the expected signal after the full amplitude has been reached in the case of the modulated cw laser (respectively train of laser pulses) with a continuous monitoring of the pendulum over a time of one week. Moreover, due to the large  $Q_{\text{eff}}$ , the times of order  $2\pi Q_{\text{eff}}/\omega_0$  required to reach the quoted maximum amplitude of the sensor become forbidding large (about 4782 days with the above values). Reducing the driving time to about 1 week reduces the amplitude by a factor  $\sim 218$  (as the amplitude builds up like  $\sim (1 - e^{-\omega_0 t/(2Q_{\text{eff}})})$ ). After that time, and assuming  $\beta \simeq 1$ , with a measurement time of one week, the sensitivity of a single detector is about a factor 33,700 too small to measure the signal produced by the cw cavity.

## 2. LHC beam

The minimum frequency of one bunch of ultra-relativistic protons going around the ring of the LHC is in the kHz range (see Sec.IIB). Lower frequencies could be achieved by modulating the beam position with low frequency. The LHC as a source is expected to create almost 20 times larger amplitude than the considered cw-pumped cavity, due to the higher pulse power  $P_p = P_{\text{avg}}^{\text{LHC}}$  where an “on-off” modulation of the LHC beam, similar to the cw cavity pumping scheme was assumed. After one week of build up time and one week of measurement time one would be about a factor 1,800 off from measuring the signal with a single detector. Substantially more development will be needed to bridge this gap. Ideas in this direction are developed in the next section.

### 3. Optimized Pendulum Setup

According to eq.(5.60) in [66] the total position-noise power at frequency  $\omega$  of a harmonic oscillator with (undamped) resonance frequency  $\Omega$  measured with a transducer and amplifier that add back-action noise (referred back to the input) can be written as

$$\bar{S}_{\text{xx,tot}}(T, \omega, \Omega, Q, m) = \frac{\gamma_0}{\gamma_0 + \gamma} \bar{S}_{\text{xx,eq}}(T, \omega, \Omega, Q, m) + \bar{S}_{\text{xx,add}}(T, \omega, \Omega, Q, m) \quad (27)$$

where  $\gamma_0$  is the intrinsic oscillator damping without coupling to the transducer and  $\gamma \equiv \gamma(\omega)$  the damping with the coupling. The equilibrium noise (comprising both quantum noise and thermal noise at temperature  $T$ ) can be written as

$$\bar{S}_{\text{xx,eq}}(T, \omega, \Omega, Q, m) = \hbar \coth \left( \frac{\hbar \omega}{2k_B T} \right) \text{Im} \chi_{\text{xx}}(\omega, \Omega, Q, m) \quad (28)$$

$$\text{Im} \chi_{\text{xx}}(\omega, \Omega, Q, m) = \frac{Q \omega \Omega}{m(\omega^2 \Omega^2 + Q^2(\omega^2 - \Omega^2)^2)}, \quad (29)$$

with the quality factor  $Q \equiv \Omega/(\gamma_0 + \gamma)$ . To calculate  $\bar{S}_{\text{xx,add}}$ , one needs to know the force noise power of the detector and amplifier, but  $\bar{S}_{\text{xx,add}}$  is lower bounded by  $\bar{S}_{\text{xx,addMin}} = \hbar |\text{Im} \chi_{\text{xx}}|$ . With this lowest possible value and the replacements  $\Omega \rightarrow \omega_0$ ,  $Q \rightarrow Q_{\text{eff}}$ ,  $T \rightarrow T_{\text{eff}}$ , one obtains for the total noise power to lowest order in  $\gamma/\gamma_0$  (which slightly overestimates the contribution from  $\bar{S}_{\text{xx,eq}}(T, \omega, \Omega, Q, m)$ )

$$\bar{S}_{\text{xx,tot}} = \hbar \left( 1 + \coth \left( \frac{\hbar \omega}{2k_B T_{\text{eff}}} \right) \right) \text{Im} \chi_{\text{xx}}(\omega, \omega_0, Q_{\text{eff}}, m). \quad (30)$$

The maximum amplitude  $x_{\text{grav}}$  of the pendulum is given by eq.(26) with  $\sin(\tau_p \omega_0/2) = 1$ , but is reached only asymptotically as function of time, namely as  $x_{\text{grav}}(t) = x_{\text{grav}}(1 - \exp(-\omega_0 t/(2Q_{\text{eff}})))$ . We assume that the total time  $\tau_{\text{tot}} = 1$  week for the experiment is split as  $\tau_{\text{tot}} = \tau_r + \tau_m$  into a time  $\tau_r$  needed for the amplitude of the pendulum to rise to a certain level, and a measurement time  $\tau_m$  used for reducing the noise. This could be improved upon in practice with corresponding modeling. The total signal to noise ratio on resonance is then given by

$$\begin{aligned} S/N &= x_{\text{grav}} (1 - \exp(-\omega_0(\tau_{\text{tot}} - \tau_m)/(2Q_{\text{eff}}))) \frac{\sqrt{\tau_m}}{\sqrt{\bar{S}_{\text{xx,tot}}}} \\ &\simeq 0.01 \frac{g}{s^{3/2}} \frac{(1 - e^{((\tau_m - \tau_{\text{tot}})\frac{\omega_m^2}{2Q_m \omega_0})}) \sqrt{Q_m m \tau_m}}{\omega_m \sqrt{1 + \coth \frac{2 \cdot 10^{-11} Q_m \omega_0^3}{\omega_m^2}}}, \end{aligned} \quad (31)$$

where in (31) an initial temperature of 50 mK (reachable by a dilution fridge) was assumed, and a distance  $\rho = 200 \mu\text{m}$  of the center of mass of the pendulum from the beam axis. All quantities are in SI units. From that equation it is evident that the mass  $m$  should be as large as possible. At the same time,  $m$  cannot be made arbitrarily large, as otherwise the distance from the beam axis would have to be increased as well, which would lead to a decay of the signal  $\propto 1/\rho$  for  $\rho \gg \rho_{\min}$ , where  $\rho_{\min}$  is the minimum distance from the beam axis (which might contain a shielding of the particle beam in the case of the LHC, and which we assume to be  $\rho_{\min} = 100 \mu\text{m}$  for the LHC). In principle, for a spherical pendulum body, a scaling  $\propto m^{1/6}$  would still result, but it turns out that unrealistically large masses (larger than 1 kg) would be needed before this scaling gives an advantage over an alternative design with a cylindrical pendulum body that allows to maintain  $\rho = 200 \mu\text{m}$ . If we allow that cylinder to become as long as  $L_{\text{cyl}} = 0.5 \text{ m}$  and determine the maximum mass as  $m = 0.9\pi\varrho_{\text{Si}}(\rho - \rho_{\min})^2 L_{\text{cyl}}$  (where 0.9 is a “fudge factor” that avoids that the pendulum touches the shielding), we find  $m = 33 \text{ mg}$ .

With that value inserted in eq.(31), one can optimize  $S/N$  with respect to the parameters  $\tau, \omega_m, \omega_0, Q_m$ . In the range  $10^{-3}/\text{s} \leq \omega_m, \omega_0 \leq 10^4/\text{s}$ ,  $10^3 \leq Q_m \leq 10^6$ , a maximum value  $S/N \simeq 0.27$  is found for  $\tau_m = 2.4 \cdot 10^5 \text{ s}$ ,  $\omega_m = 2\pi \cdot 1.8 \text{ Hz}$ ,  $\omega_0 = 2\pi \cdot 50.3 \text{ Hz}$ , and  $Q_m = 1.3 \cdot 10^5$ . Remarkably, the optimal value for  $\omega_m$  is very close to the one for the existing pendulum in [1], but both  $\omega_0$  and  $Q_m$  are substantially smaller than what was achieved already. This is linked to the fact that for very large  $Q_{\text{eff}}$  the signal rises very slowly. Nevertheless, even with these parameters the temperature scaling leads to a temperature of the cooled mode of about 1.9 nK, substantially below the few  $\mu\text{K}$  expected in [68], and it remains to be seen whether this is realistic.

A signal to noise ratio of 0.27 is still not good enough, but the planned upgrade of the LHC to the high-luminosity LHC [54] should increase  $S/N$  by a factor 10. Another factor 2.9 is expected to be gained by switching to tungsten (with mass density  $\varrho_W = 19,250 \text{ kg/m}^3$ ) as pendulum material, all other optimized parameters remaining equal. Both factors combined lead to a  $S/N \simeq 7.7$ .

The found maximum of  $S/N$  is rather flat, especially with respect to the quality factor, such that there is a wide range of values with similar signal to noise ratios that allow one

|                    | rod  |  | liquid helium  |  | monolithic pendulum <sup>□</sup>                     |
|--------------------|--|--|--|--|--|
| $\omega_0$         | $2\pi \cdot 10^3$ Hz                                 |  | $2\pi \cdot 10^9$ Hz                                 |  | $2\pi \cdot 2.8 \cdot 10^3$ Hz                       |
| sensitivity        | $1 \cdot 10^{-17} \frac{\text{m}}{\sqrt{\text{Hz}}}$ | $4 \cdot 10^{-17} \frac{\text{m}}{\sqrt{\text{Hz}}}$ | $2 \cdot 10^{-17} \frac{\text{N}}{\sqrt{\text{Hz}}}$ | $1 \cdot 10^{-12} \frac{\text{m}}{\sqrt{\text{Hz}}}$ | $8 \cdot 10^{-13} \frac{\text{m}}{\sqrt{\text{Hz}}}$ |
| limiting factor    | thermal noise  |  | SQL  |  | SQL  |
| expected amplitude |  |  |  |  |  |
| laser pulses       | $2 \cdot 10^{-25}$ m                                 | $2 \cdot 10^{-34}$ m                                 | $2 \cdot 10^{-25}$ N                                 | $1 \cdot 10^{-20}$ m                                 | $4 \cdot 10^{-18}$ m                                 |
| cw cavity          | $4 \cdot 10^{-25}$ m                                 | $4 \cdot 10^{-34}$ m                                 | $3 \cdot 10^{-25}$ N                                 | $2 \cdot 10^{-20}$ m                                 | $7 \cdot 10^{-18}$ m                                 |
| LHC beam *         | $8 \cdot 10^{-24}$ m                                 | $9 \cdot 10^{-32}$ m                                 | $7 \cdot 10^{-24}$ N                                 | $4 \cdot 10^{-19}$ m                                 | $1 \cdot 10^{-16}$ m                                 |

Table II. Comparison of the estimated sensitivity of the listed detectors with the expected amplitude of the sources considered on resonance and after the full build-up-time of the detector's oscillation. For the cases in which the main limiting factor is thermal noise, a temperature of 5 mK was assumed. Other parameters see text.

<sup>□</sup> The values are calculated for the monolithic pendulum from [1] at  $\omega_0 = 2\pi \cdot 1$  kHz.

\* assuming the LHC beam can be modulated to produce a signal with appropriate frequency while maintaining the same average power.

to take into account other engineering constraints not considered here. Hence, with the high-luminosity LHC and an optimized pendulum there is realistic hope that GR could be tested for the first time in this ultra-relativistic regime with a controlled terrestrial source and adapted optimized detector. Without the upgrade of the LHC, further improvements from using a multitude of detectors (and possibly coherent averaging by coupling them all to the same read-out cavity) or longer integration times can be envisaged that would also bring  $S/N$  to order one.

## IV. DISCUSSION

### A. Perspectives for measuring the gravitation of light or particle beams

Pulsed light or particle beams are high intensity sources for periodic gravitational fields on a laboratory scale. Both light- and particle beams result in very similar energy-momentum tensors including off-diagonal components in Cartesian coordinates,  $T_{03} = T_{30} = T_{00}$  for

propagation in  $z$ -direction, characteristic of the ultra-relativistic regime in the sense of special relativity. The resulting gravitational effects can still be calculated within linearized gravity and the effective Newtonian potential as experienced by a non relativistic sensor is equivalent to that of a long and thin rod. For relativistic test particles, the more complicated structure of the metric tensor entails additional effects.

We investigated three concrete examples: For laser beams we considered femtosecond pulse lasers with pulses fed into a high finesse cavity, where they oscillate to and fro with a frequency in the GHz range; and similarly, cw lasers used to pump a cavity periodically. For particle beams, we considered the Large Hadron Collider (LHC) with its beam of proton bunches flying along the accelerator ring. All sources considered lead to oscillating curvatures of space-time and acceleration of test particles with precisely controlled frequency up to the GHz range. In addition, it should be possible to modulate these signals with much lower frequency, down to the kHz regime. One way of achieving this for pulsed lasers is to fill the cavity successively with pulses, such that in the end half of the cavity is filled, the other half empty. For the cavity pumped by a cw laser, the pumping period should be easily adjustable to lower frequencies. For the LHC a periodical modulation of the spatial position of the beam could produce a lower frequency signal. Well defined and tunable frequencies offer the potential for purpose built mechanical oscillators as detectors. If the low-frequency modulation of the particle density or beam position can be achieved, the LHC is the most promising ultrarelativistic source of gravity with a gravitational field strength 20 times stronger than the laser sources considered here. We considered three simple detector setups: A deformable rod offers force accumulation along its length thanks to its Young modulus. However, the spatial decrease of the studied gravitational effects limits the effects of force accumulation, resulting in immeasurably small amplitudes of the order  $8 \cdot 10^{-24} \text{ m}$  even in the case of the LHC as a source.

In the liquid helium chamber from Singh et al. [67], very high quality factors and low noise allow for sound wave buildup within the chamber. To use it as a sensor for the gravitational field of high power laser light or the LHC beam, one has to modulate the beams with frequencies in the kHz range. With the numbers from the prototype of Singh et al. [67], the gravitational force for the LHC is 3.5 orders of magnitude below the detectability limit of this detector with an averaging time of one week.

In the end, a pendulum from [1] turned out to be the most promising detector. In its

present form the fully built-up signal from the LHC is about 4 orders of magnitude away from the sensitivity achievable within 1 s of averaging time, but by optimizing the design a signal to noise ratio of about 0.27 can be achieved within one week of signal rise time and averaging. By building the pendulum from a denser material such as tungsten and profiting from the planned high-luminosity upgrade of the LHC a  $S/N \simeq 7$  appears possible with one week of measurement time. Very high source frequencies (GHz) turned out to be detrimental rather than instrumental to the detectability of gravitational accelerations with the detectors considered. In particular, the pendulum detector in its current design [1] needs a source oscillating with a frequency of the order of 400 Hz to kHz, the superfluid helium detector a frequency of order kHz. Operating the pendulum at higher frequencies might be possible and relatively easy to achieve, given that the relevant noise terms in the kHz range stem from suspension eigenmodes, which are changeable by design. Also in [77] parametric cooling into the ground state for pendulum style gravitational sensors was demonstrated, reducing problems from thermal noise and seismic noise in an even larger frequency range.

Our considerations concerned fundamental limitations so far, so that a  $S/N$  ratio larger than 1 should be considered a necessary condition, but would still make for a very difficult experiment with additional noise and engineering issues to be overcome.

## B. Perspectives for quantum gravity experiments

The realization that the gravitational effect of light or high-energy particle beams might become measurable in the near future opens new experimental routes to quantum gravity, in the sense that it might become possible to study gravity of light or matter in a non-trivial quantum superposition. Concerning light, non-classical states of light, in particular in the form of squeezed light, have been studied and experimentally realized for a long time, and are now used for enhanced gravitational-wave-sensing in LIGO [78]. While the current records of squeezing were obtained for smaller intensities than relevant for the gravitational sources we consider here [79], squeezing and entanglement shared by many modes was already achieved for photon numbers on the order  $10^{16}$  by using a coherent state in one of the modes [80]. This is substantially smaller than the  $\sim 10^{21}$  photons estimated in the cavity in the example of the cw laser leading to 100 GW circulating power considered above, but one might hope that technology progresses to achieve at least a small amount of squeezing also for the high-power

sources relevant here.

As for the high-energy particle beams, transverse “coherent oscillations” of two colliding accelerator beams (including the ones at LHC) have already been studied [81–85] but these are of classical nature. Non-trivial quantum states of the beam are those that cannot be described by a positive semidefinite Glauber-Sudarshan  $P$ -function, a concept from quantum optics that is well established for harmonic oscillators and is hence applicable to small-amplitude transverse motion of the particle beam in the focusing regions where there is a linear restoring force. A stronger requirement would be a non-positive-semidefinite Wigner function, which can be applied to any system with a phase space. In order to reach such quantum states, it will be necessary to cool the particle beams. Efforts to do so are on the way or proposed for other motivations: Cooling enhances the phase space density and hence the intensity of the beam in its center. In addition, new phases of matter in the form of classical crystalline beams attracted both theoretical and experimental interest at least since the 1980s [86–92]. Recently it was proposed to extend this work to create an “ultracold crystalline beam” and turning an ion beam into a quantum computer. For this, the beam should become an ion Coulomb crystal cooled to such low temperatures that the de Broglie wavelength becomes larger than the particles’ thermal oscillation amplitudes [93]. Ideally, for our purposes, the center-of-mass motion of the beam should be cooled to the ground state of the (approximate) harmonic oscillator that restrains locally, at the detector position, the transverse motion, before interesting quantum superpositions can be achieved.

However, even non-trivial superpositions in longitudinal direction would create an experimental situation for which there is currently no established theory for calculating the gravitational effect. Different techniques for cooling particle beams are available (see e.g. [94, 95] for overviews): Stochastic cooling (measurement of deviation from the ideal beam-line and fast electronic counter-measures further down the beamline) was used at CERN for producing high-intensity anti-proton beams from 1972 till 2017 and is still used there for anti-proton deceleration, as well as at Forschungszentrum Jülich (COSY experiment) and GSI Helmholtzzentrum für Schwerionenforschung GmbH (Heavy Ion storage ring ESR); electron cooling (absorption of entropy by a co-propagating electron beam of much lower energy and entropy), and a modern cousin of it, “coherent electron cooling” [96], under development at Brookhaven National Lab for ion energies up to 40 GeV/u for  $\text{Au}^{+79}$  ions [55, 97]; and laser cooling, with which longitudinal temperatures on the order of mK have been reached

for moderately relativistic ion beams [98, 99]. Laser cooling is most efficient for longitudinal cooling, but transverse cooling can be achieved to some extent through sympathetic cooling [100]. Laser cooling is now proposed for an ultrarelativistic heavy-ion upgrade of the LHC [54]. Despite all these techniques, ground states of the transverse center-of-mass motion have never been reached in any ultra-relativistic particle beam as far as we know, nor was it perceived as an important goal. We hope that the perspective of winning the race to the first quantum gravity experiment will change this. As Grishchuk put it [12]: “The laboratory experiment is bound to be expensive, but one should remember that a part of the cost is likely to be reimbursed from the Nobel prize money †. The successful development of ion-trap quantum computers, where ground-state cooling of collective modes of ion crystals has become standard, might lend credibility to the feasibility of the endeavor.

*Acknowledgments:* DB thanks Daniel Estève for discussion, correspondence and references, and for proposing the idea to look at pulses in a cavity; and Werner Vogelsang for a discussion on particle accelerator beams. DR would like to thank the Humboldt Foundation for supporting his work with their Feodor Lynen Research Fellowship and the European Commission’s Marie Skłodowska-Curie Actions for support via the Individual Fellowship.

## Appendix A: Gravitational field of a laser-pulse in a cavity

Following the calculation of the gravitational field of a box shaped laser pulse of length  $L$  emitted at  $z = 0$  and absorbed at  $z = D$  from [17, 20] we extend the calculation to an oscillation of a short pulse ( $L < D$ ) between 0 and  $D$ . For a pulse propagating along the  $\pm z$ -direction the energy momentum tensor is given by  $T_{00} = T_{zz} = \mp T_{0z} = \mp T_{z0} = u(z, t)\delta(x)\delta(y)A$ , where  $u(z, t)$  is the energy density of the electromagnetic field in 3D and  $A$  is the effective transverse area. This energy momentum tensor violates the continuity equation as the recoil of the mirrors is neglected. However, ultimately only positions very close to the beam will be considered where these contributions vanish. For a more complete consideration the Vaidya metric [101] would have to be used. Similar considerations imply that the effect persists, but calculations are more complicated. The energy density is given by

$$u(z, t) = u_p \Theta(z)\Theta(D - z) \sum_{n=0}^{\infty} (\chi_+^n(z, t) + \chi_-^n(z, t)), \quad (\text{A1})$$

where

$$\chi_+^n(z, t) = \left( \Theta(ct - 2nD - z) - \Theta(ct - 2nD - z - L) \right) \quad (\text{A2})$$

$$\chi_-^n(z, t) = \left( \Theta(ct - (2n+1)D + (z - D)) - \Theta(ct - (2n+1)D + (z - D) - L) \right) \quad (\text{A3})$$

delimit the profile of the pulse injected at  $t = 0$  and reflected  $2n$  times ( $2n+1$  times) traveling in positive (negative)  $z$ -direction, and  $u_p = \frac{E_p}{LA}$  is the pulse energy density.

From the wave equation in the Lorenz gauge

$$\square h_{\mu\nu} = -\frac{16\pi G}{c^4} T_{\mu\nu} \quad (\text{A4})$$

the metric perturbation can be calculated using the Green's function

$$h_{\mu\nu}(\mathbf{r}, t) = \frac{4G}{c^4} \int d^3r' \frac{T_{\mu\nu}(\mathbf{r}', t - |\mathbf{r} - \mathbf{r}'|/c)}{|\mathbf{r} - \mathbf{r}'|}. \quad (\text{A5})$$

Given the energy-momentum tensor, the metric perturbation can be decomposed into  $h_{\mu\nu} = h_{\mu\nu}^+ + h_{\mu\nu}^-$  and the only non-zero elements of  $h_{\mu\nu}^\pm$  are  $h_{00}^\pm = h_{zz}^\pm = \mp h_{z0}^\pm = \mp h_{0z}^\pm \equiv h^\pm$ , with

$$h^\pm(x, y, z, t) = \frac{4Gu_p A}{c^4} \int_0^D dz' \frac{\sum_n \chi_\pm^n(z', t - \sqrt{\rho^2 + (z - z')^2}/c)}{\sqrt{\rho^2 + (z - z')^2}}, \quad (\text{A6})$$

$$\rho = \sqrt{x^2 + y^2}, \text{ and } u_p A = \frac{P}{c}.$$

The box function  $\chi_+^n$  imposes the additional boundaries of  $a_+^n < z' < b_+^n$ , with

$$a_+^n = z + \frac{(ct - 2nD - L - z)^2 - \rho^2}{2(ct - 2nD - L - z)} \quad (\text{A7})$$

$$b_+^n = z + \frac{(ct - 2nD - z)^2 - \rho^2}{2(ct - 2nD - z)}. \quad (\text{A8})$$

Similarly, the box function  $\chi_-^n$  adds the constraints of  $a_-^n < z' < b_-^n$ , with

$$b_-^n = z - \frac{(ct - (2n+1)D - L + (z - D))^2 - \rho^2}{2(ct - (2n+1)D - L + (z - D))} \quad (\text{A9})$$

$$a_-^n = z - \frac{(ct - (2n+1)D + (z - D))^2 - \rho^2}{2(ct - (2n+1)D + (z - D))}. \quad (\text{A10})$$

Following [20] the substitution  $\zeta(z') = z' - z + \sqrt{\rho^2 + (z' - z)^2}$  is used to further simplify

the integration. The constraints turn into

$$\zeta(0) = r - z \quad (\text{A11})$$

$$\zeta(D) = r_D - (z - D) \quad (\text{A12})$$

$$\zeta(a_+^n) = ct - 2nD - L - z \quad (\text{A13})$$

$$\zeta(b_+^n) = ct - 2nD - z \quad (\text{A14})$$

$$\zeta(b_-^n) = \frac{\rho^2}{ct - (2n+1)D - L + (z - D)} \quad (\text{A15})$$

$$\zeta(a_-^n) = \frac{\rho^2}{ct - (2n+1)D + (z - D)}, \quad (\text{A16})$$

where  $r = \sqrt{\rho^2 + z^2}$ , and  $r_D = \sqrt{\rho^2 + (z - D)^2}$ .

For an observer positioned at  $z \in (L, D - L)$  there are 4 different space-time zones

$$P_0^n: 2nD < ct - r < 2nD + L$$

causally connected to the reflection at  $z = 0, ct = 2nD$

$$\triangleright^n: 2nD + r + L < ct < (2n+1)D + r_D$$

not causally connected to any reflection events, but causally connected to the pulse traveling from  $z = 0, ct = 2nD$  to  $z = D, ct = (2n+1)D$

$$P_D^n: (2n+1)D < ct - r_D < (2n+1)D + L$$

causally connected to the reflection at  $z = D, ct = (2n+1)D$

$$\triangleleft^n: (2n+1)D + r_D + L < ct < (2n+2)D + r$$

not causally connected to any reflection events, but causally connected to the pulse traveling from  $z = D, ct = (2n+1)D$  to  $z = 0, ct = (2n+2)D$ .

The metric perturbation is then given by

$$h^+ = \frac{4GP}{c^5} \begin{cases} \ln \frac{\zeta(b_+^n)}{\zeta(0)} = \ln \frac{ct_{2n}-z}{r-z} & \text{for } (z, t) \in P_0^n, \\ \ln \frac{\zeta(b_+^n)}{\zeta(a_+^n)} = \ln \frac{ct_{2n}-z}{ct_{2n}-L-z} & \text{for } (z, t) \in \triangleright^n, \\ \ln \frac{\zeta(D)}{\zeta(a_+^n)} = \ln \frac{r_D-(z-D)}{ct_{2n+1}-L-(z-D)} & \text{for } (z, t) \in P_D^n, \\ 0 & \text{for } (z, t) \in \triangleleft^n, \end{cases} \quad (\text{A17})$$

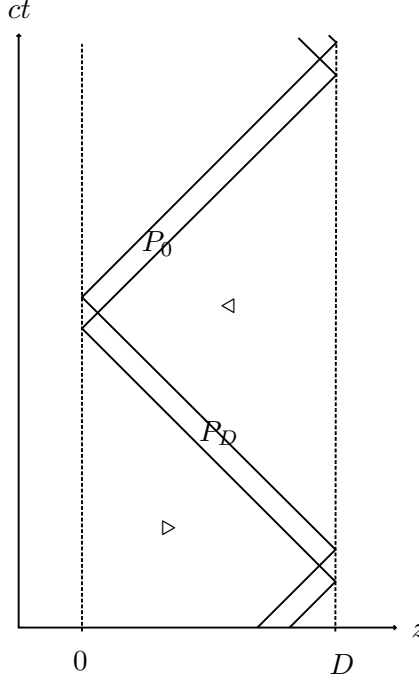


Figure 2.

caused by the pulses starting from  $z = 0$  and

$$h^- = \frac{4GP}{c^5} \begin{cases} \ln \frac{\zeta(b_-^{n-1})}{\zeta(0)} = \ln \frac{\rho^2}{(ct_{2n}-L+z)(r-z)} & \text{for } (z, t) \in P_0^n, \\ 0 & \text{for } (z, t) \in \triangleright^n, \\ \ln \frac{\zeta(D)}{\zeta(a_-^n)} = \ln \frac{(r_D-(z-D))(ct_{2n+1}+(z-D))}{\rho^2} & \text{for } (z, t) \in P_D^n, \\ \ln \frac{\zeta(b_-^n)}{\zeta(a_-^n)} = \ln \frac{ct_{2n+1}+(z-D)}{ct_{2n+1}-L+(z-D)} & \text{for } (z, t) \in \triangleleft^n, \end{cases} \quad (\text{A18})$$

caused by the pulses returning from  $z = D$ , where  $t_j := t - jD/c$ .

Following [20], the only independent non-vanishing elements of the Riemann curvature tensor are given by

$$R_{0z0z} = -\frac{1}{2} \left( \frac{1}{c} \partial_t + \partial_z \right)^2 h^+ - \frac{1}{2} \left( \frac{1}{c} \partial_t - \partial_z \right)^2 h^- \quad (\text{A19})$$

$$R_{0z0i} = -R_{0zzi} = -\frac{1}{2} \partial_i \left( \frac{1}{c} \partial_t + \partial_z \right) h^+ - \frac{1}{2} \partial_i \left( \frac{1}{c} \partial_t - \partial_z \right) h^- \quad (\text{A20})$$

$$R_{0i0j} = R_{zizj} = -\frac{1}{2} \partial_i \partial_j (h^+ + h^-) \quad (\text{A21})$$

$$R_{0izj} = \frac{1}{2} \partial_i \partial_j (h^+ - h^-), \quad (\text{A22})$$

where  $i, j \in \{x, y\}$ .

Given the explicit form of  $h^+$  and  $h^-$  from eqs.(A17) and (A18), the curvature is

$$P_0^n: R_{0z0z} = \frac{4GP}{c^5} \frac{z}{r^3}, \quad R_{0z0i} = 0, \quad R_{0i0j} = \frac{4GP}{c^5} \frac{z}{\rho^2 r} \left( \delta_{ij} - \frac{r_i r_j}{\rho^2 r^2} (2r^2 + \rho^2) \right), \quad R_{0izj} = -\frac{4GP}{c^5} \frac{1}{\rho^2} \left( \delta_{ij} - \frac{2r_i r_j}{\rho^2} \right)$$

$$\triangleright^n: R_{\mu\nu\rho\sigma} = 0 \quad \forall \mu, \nu, \rho, \sigma$$

$$P_D^n: R_{0z0z} = \frac{4GP}{c^5} \frac{D-z}{r_D^3}, \quad R_{0z0i} = 0, \quad R_{0i0j} = \frac{4GP}{c^5} \frac{(D-z)}{r_D \rho^2} \left( \delta_{ij} - \frac{r_i r_j}{r_D^2 \rho^2} (2r_D^2 + \rho^2) \right), \quad R_{0izj} = \frac{4GP}{c^5} \frac{1}{\rho^2} \left( \delta_{ij} - \frac{2r_i r_j}{\rho^2} \right)$$

$$\triangleleft^n: R_{\mu\nu\rho\sigma} = 0 \quad \forall \mu, \nu, \rho, \sigma.$$

In the limit  $\rho \ll r, r_D$ , the only independent components of the curvature in leading order are

$$R_{0i0j} = -R_{0izj} = \frac{4GP}{c^5} \frac{1}{\rho^2} \left( \delta_{ij} - 2 \frac{r_i r_j}{\rho^2} \right) \equiv \mathcal{R} \quad \forall (z, t) \in P_0^n \quad (\text{A23})$$

$$R_{0i0j} = \mathcal{R} = R_{0izj} \quad \forall (z, t) \in P_D^n, \quad (\text{A24})$$

with  $\rho \ll z, z - D$ . A simplified metric perturbation resulting in the same curvature tensor as equation (A23) is given by

$$\tilde{h}^+ = \begin{cases} -\frac{8GP}{c^5} \ln \rho & \text{for } (z, t) \in P_0^n \\ 0 & \text{else} \end{cases}, \quad \tilde{h}^- = \begin{cases} -\frac{8GP}{c^5} \ln \rho & \text{for } (z, t) \in P_D^n \\ 0 & \text{else} \end{cases}. \quad (\text{A25})$$

The geodesic equation for a test particle particle at position  $x^\mu$  is given in coordinate time  $t = \frac{1}{c}x^0$  by

$$\frac{d^2 x^\mu}{dt^2} = -\Gamma_{\alpha\beta}^\mu \frac{dx^\alpha}{dt} \frac{dx^\beta}{dt} + \Gamma_{\alpha\beta}^0 \frac{dx^\alpha}{dt} \frac{dx^\beta}{dt} \frac{dx^\mu}{dt} \quad (\text{A26})$$

For a non-relativistic test particle this reduces to

$$\ddot{x}^a = -c^2 \Gamma_{00}^a + \mathcal{O} \left( \frac{v^2}{c^2} \right), \quad (\text{A27})$$

with the linearized Christoffel symbol

$$\Gamma_{\mu\nu}^\rho = \frac{1}{2} \eta^{\lambda\rho} (\partial_\mu h_{\nu\lambda} + \partial_\nu h_{\lambda\mu} - \partial_\lambda h_{\mu\nu}) \implies \Gamma_{00}^a = -\frac{1}{2} \partial_a \tilde{h}_{00}. \quad (\text{A28})$$

The acceleration a non-relativistic sensor experiences is therefore equivalent to that from a Newtonian potential

$$\Phi = \frac{4GP}{c^3} \ln \rho \quad (\text{A29})$$

for the duration of the pulse passing by  $(P_0, P_D)$  with the potential vanishing at all other times.

## Appendix B: Intensity in a Fabry-Pérot resonator

The considerations here follow those from [48] closely but are modified to reflect the setups used in this work.

For a Fabry-Pérot resonator consisting of two mirrors with field reflection coefficients  $\sqrt{R_1}, \sqrt{R_2}$  and field transmission coefficients  $\sqrt{T_1}, \sqrt{T_2}$  the field in cavity (at the face of mirror 1) resulting from a pump beam striking mirror 1 can be written as

$$E_{\text{cav}}(t) = \sqrt{R_1 R_2} E_{\text{cav}}(t - \tau_{\text{rt}}) + \sqrt{T_1} E_{\text{pump}}(t) \quad (\text{B1})$$

in the time domain, where  $\tau_{\text{rt}}$  is the time for one round trip in the cavity. In the frequency domain this can be written as

$$\tilde{E}_{\text{cav}}(\omega) = \tilde{G}(\omega) \tilde{E}_{\text{pump}}(\omega), \text{ with } \tilde{G}(\omega) = \frac{\sqrt{T_1}}{1 - \sqrt{R_1 R_2} e^{-i\omega\tau_{\text{rt}}}}. \quad (\text{B2})$$

### 1. Single monochromatic rectangular pulse

For a monochromatic pump field of frequency  $\omega_E$  and length  $\tau_p$  entering the cavity at  $t = 0$  the pump field is given by

$$E_{\text{pump}}^p(t) = E_0 e^{i\omega_E t} \mathbb{U}_{\tau_p}(t), \text{ with } \mathbb{U}_{\tau_p}(t) = \Theta(t) - \Theta(t - \tau_p) \quad (\text{B3})$$

$$\Rightarrow \tilde{E}_{\text{pump}}^p(\omega) = E_0 \tau_p e^{-i\omega\tau_p/2} \text{sinc}((\omega - \omega_E)\tau_p). \quad (\text{B4})$$

The corresponding Fourier transformed field amplitude in the cavity is then given through eq.(B2) by

$$\tilde{E}_{\text{cav}}^p(\omega) = E_0 \frac{\sqrt{T_1} e^{-i\omega\tau_p/2}}{1 - \sqrt{R_1 R_2} e^{-i\omega\tau_{\text{rt}}}} \tau_p \text{sinc}((\omega - \omega_E)\tau_p) \quad (\text{B5})$$

$$\Rightarrow E_{\text{cav}}^p(t) = E_0 \sqrt{T_1} \sum_{n=0}^{\infty} \sqrt{R_1 R_2}^n e^{i\omega_E(t - n\tau_{\text{rt}})} \mathbb{U}_{\tau_p}(t - n\tau_{\text{rt}}) \quad (\text{B6})$$

For a very short pulse  $\tau_p \ll \tau_{\text{rt}}$  none of the addends will overlap and the intensity in the cavity is

$$I_{\text{cav}}^p(t) = |E_{\text{cav}}^p(t)|^2 = E_0^2 T_1 \sum_{n=0}^{\infty} (R_1 R_2)^n \mathbb{U}_{\tau_p}(t - n\tau_{\text{rt}}). \quad (\text{B7})$$

The pulse enters the cavity with an intensity reduced by  $T_1$  and is reduced by a further factor  $R_1 R_2$  for each subsequent round trip. The average power in the cavity relative to

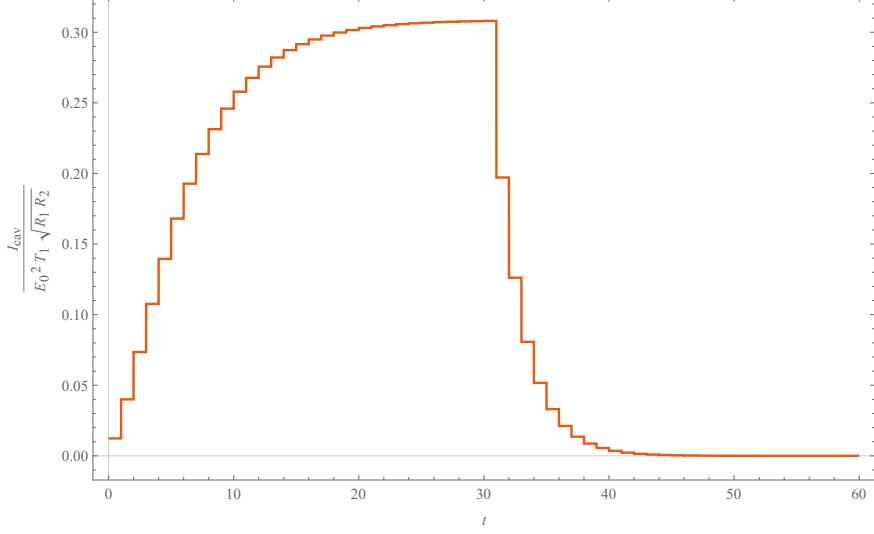


Figure 3. Intensity inside the cavity resulting from a long ( $\tau_p \gg \tau_{rt}$ ) rectangular pulse of monochromatic or spectrally narrow light.

that of the pump laser is then given by

$$\frac{P_{\text{cav}}}{P_0} = T_1 \sum_{n=0}^{\infty} (R_1 R_2)^n = \frac{T_1}{1 - R_1 R_2} = \frac{1 - R_1}{1 - R_1 R_2} \lesssim 1. \quad (\text{B8})$$

For long pulses ( $\tau_p \gg \tau_{rt}$ ) and a resonant cavity ( $\omega_E \tau_{rt} = 2\pi m$ ) only addends from  $n_{\min} = \max \left( 0, \left\lceil \frac{t - \tau_p}{\tau_{rt}} \right\rceil \right)$  to  $n_{\max} = \max \left( 0, \left\lfloor \frac{t}{\tau_{rt}} \right\rfloor \right)$  contribute for any given time, returning

$$E_{\text{cav}}^p(t) = E_0 \sqrt{T_1} \left[ \frac{1 - \sqrt{R_1 R_2}^{n_{\max}+1}}{1 + \sqrt{R_1 R_2}} - \frac{1 - \sqrt{R_1 R_2}^{n_{\min}+1}}{1 + \sqrt{R_1 R_2}} \right] \quad (\text{B9})$$

$$= E_0 \sqrt{T_1} \sqrt{R_1 R_2} \frac{\sqrt{R_1 R_2}^{n_{\min}} - \sqrt{R_1 R_2}^{n_{\max}}}{1 + \sqrt{R_1 R_2}}. \quad (\text{B10})$$

The intensity for this long-pulse resonant cavity case can be described as a “jagged shark fin” and is plotted in fig. 3

## 2. Series of monochromatic rectangular pulses

A series of periodic pulses separated by time  $\tau_{rt}$  can be written as a sum of pulses  $E_{\text{pump}}^{\Sigma}(t) = \sum_k E_{\text{pump}}^p(t - k\tau_{\text{rep}})$ . As all of the operations on the field are linear the pump field eq. (B5) can be used to find

$$E_{\text{cav}}^{\Sigma}(t) = \sum_k E_{\text{cav}}^p(t - k\tau_{\text{rep}}). \quad (\text{B11})$$

For repetition times much longer than the life time of a pulse in the cavity  $\tau_L \sim \frac{\tau_{\text{rt}}(R_1 R_2)^{1/4}}{1 - \sqrt{R_1 R_2}}$  and  $\tau_p$  the addends barely overlap such that there is no interference between consecutive pulses. In this case the intensity in the cavity is just that of the singular pulse repeating periodically.

---

- [1] S. B. Cataño Lopez, J. G. Santiago-Condori, K. Edamatsu, and N. Matsumoto, High- $q$  milligram-scale monolithic pendulum for quantum-limited gravity measurements, *Phys. Rev. Lett.* **124**, 221102 (2020).
- [2] E. Berti, K. Yagi, and N. Yunes, Extreme gravity tests with gravitational waves from compact binary coalescences:(i) inspiral–merger, *General Relativity and Gravitation* **50**, 1 (2018).
- [3] J. B. Jiménez, L. Heisenberg, G. J. Olmo, and D. Rubiera-Garcia, Born–infeld inspired modifications of gravity, *Physics Reports* **727**, 1 (2018).
- [4] D. Langlois, R. Saito, D. Yamauchi, and K. Noui, Scalar-tensor theories and modified gravity in the wake of gw170817, *Phys. Rev. D* **97**, 061501 (2018).
- [5] C. Barceló, R. Carballo-Rubio, and L. J. Garay, Gravitational wave echoes from macroscopic quantum gravity effects, *Journal of High Energy Physics* **2017**, 54 (2017).
- [6] A. Maselli, P. Pani, V. Cardoso, T. Abdelsalhin, L. Gualtieri, and V. Ferrari, Probing planckian corrections at the horizon scale with lisa binaries, *Phys. Rev. Lett.* **120**, 081101 (2018).
- [7] L. Grishchuk and M. Sazhin, Emission of gravitational waves by an electromagnetic cavity, *JETP* **38**, 215 (1974).
- [8] L. Grishchuk and M. Sazhin, Excitation and detection of standing gravitational waves, *JETP* **41**, 787 (1975).
- [9] L. P. Grishchuk, Gravitational waves in the cosmos and the laboratory, *Soviet Physics Uspekhi* **20**, 319 (1977), publisher: IOP Publishing.
- [10] M. Portilla and R. Lapidra, Generation of high frequency gravitational waves, *Physical Review D* **63**, 044014 (2001).
- [11] R. Ballantini, P. Bernard, E. Chiaveri, A. Chincarini, G. Gemme, R. Losito, R. Parodi, and E. Picasso, A detector of high frequency gravitational waves based on coupled microwave cavities, *Classical and Quantum Gravity* **20**, 3505 (2003).

- [12] L. P. Grishchuk, Electromagnetic Generators and Detectors of Gravitational Waves (2003), arXiv: gr-qc/0306013.
- [13] V. N. Rudenko, Very High Frequency Gravitational Waves in Laboratory and Space, Gravitation and Kosmology (in Russian) **10**, 41 (2004).
- [14] R. M. L. Baker and B. S. Baker, The Utilization of High-Frequency Gravitational Waves for Global Communications, Systemics, cybernetics and informatics **10**, 8 (2012).
- [15] N. I. Kolosnitsyn and V. N. Rudenko, Gravitational Hertz experiment with electromagnetic radiation in a strong magnetic field, *Physica Scripta* **90**, 074059 (2015).
- [16] A. Füizfa, Electromagnetic Gravitational Waves Antennas for Directional Emission and Reception, arXiv:1702.06052 [gr-qc] (2018).
- [17] R. C. Tolman, P. Ehrenfest, and B. Podolsky, On the gravitational field produced by light, *Phys. Rev.* **37**, 602 (1931).
- [18] W. B. Bonnor, The gravitational field of light, *Communications in Mathematical Physics* **13**, 163 (1969).
- [19] P. C. Aichelburg and R. U. Sexl, On the gravitational field of a massless particle, *General Relativity and Gravitation* **2**, 303 (1971).
- [20] D. Rätzel, M. Wilkens, and R. Menzel, Gravitational properties of light—the gravitational field of a laser pulse, *New Journal of Physics* **18**, 023009 (2016).
- [21] R. L. Mallett, Weak gravitational field of the electromagnetic radiation in a ring laser, *Physics Letters A* **269**, 214 (2000).
- [22] J. Strohaber, Frame dragging with optical vortices, *General Relativity and Gravitation* **45**, 2457 (2013).
- [23] D. E. Cox, J. G. O'brien, R. L. Mallett, and C. Roychoudhuri, Gravitational faraday effect produced by a ring laser, *Foundations of Physics* **37**, 723 (2007).
- [24] M. O. Scully, General-relativistic treatment of the gravitational coupling between laser beams, *Physical Review D* **19**, 3582 (1979).
- [25] P. Ji, S.-T. Zhu, and W.-D. Shen, Gravitational perturbation induced by an intense laser pulse, *International journal of theoretical physics* **37**, 1779 (1998).
- [26] P. Ji and Y. Bai, Gravitational effects induced by high-power lasers, *The European Physical Journal C-Particles and Fields* **46**, 817 (2006).

- [27] F. Schneiter, D. Rätzel, and D. Braun, The gravitational field of a laser beam beyond the short wavelength approximation, *Classical and Quantum Gravity* **35**, 195007 (2018).
- [28] F. Schneiter, D. Rätzel, and D. Braun, Corrigendum: The gravitational field of a laser beam beyond the short wavelength approximation (2018 *Class. Quantum Grav.* **35** 195007), *Classical and Quantum Gravity* **36**, 119501 (2019).
- [29] F. Schneiter, D. Rätzel, and D. Braun, Rotation of polarization in the gravitational field of a laser beam—Faraday effect and optical activity, *Classical and Quantum Gravity* **36**, 205007 (2019).
- [30] P. Ji, Y. Bai, and L. Wang, Gravitational modification of the berry phase and some other effects induced by high-power lasers, *Physical Review D* **75**, 024010 (2007).
- [31] H. Balasin and H. Nachbagauer, Boosting the kerr geometry in an arbitrary direction, *Classical and Quantum Gravity* **13**, 731 (1996).
- [32] C. Lousto and N. Sánchez, The curved shock wave space-time of ultrarelativistic charged particles and their scattering, *International Journal of Modern Physics A* **5**, 915 (1990).
- [33] C. Barabés and P. Hogan, Lightlike boost of the kerr gravitational field, *Physical Review D* **67**, 084028 (2003).
- [34] K. Nakamura, H.-S. Mao, A. J. Gonsalves, H. Vincenti, D. E. Mittelberger, J. Daniels, A. Magana, C. Toth, and W. P. Leemans, Diagnostics, Control and Performance Parameters for the BELLA High Repetition Rate Petawatt Class Laser, *IEEE Journal of Quantum Electronics* **53**, 1 (2017).
- [35] L. L. N. Laboratory, National Ignition Facility User Guide 2016 <https://nifuserguide.llnl.gov/> (2016).
- [36] G. Korn, ELI whitebook (2011).
- [37] <https://home.cern/resources/faqs/facts-and-figures-about-lhc>  
<https://lhc-machine-outreach.web.cern.ch/beam.htm>.
- [38] Beam Properties GSI (2013), [https://www.gsi.de//en/work/accelerator\\_operations/accelerators/heavy\\_ion\\_synchrotron\\_sis18/beam\\_properties.htm](https://www.gsi.de//en/work/accelerator_operations/accelerators/heavy_ion_synchrotron_sis18/beam_properties.htm).
- [39] T. Westphal, H. Hepach, J. Pfaff, and M. Aspelmeyer, Measurement of Gravitational Coupling between Millimeter-Sized Masses, arXiv:2009.09546 [gr-qc, physics:physics, physics:quant-ph] (2020).

[40] K. Komori, Y. Enomoto, C. P. Ooi, Y. Miyazaki, N. Matsumoto, V. Sudhir, Y. Michimura, and M. Ando, Attoneutron-meter torque sensing with a macroscopic optomechanical torsion pendulum, *Phys. Rev. A* **101**, 011802 (2020).

[41] J. Schmöle, M. Dragosits, H. Hepach, and M. Aspelmeyer, A micromechanical proof-of-principle experiment for measuring the gravitational force of milligram masses, *Classical and Quantum Gravity* **33**, 125031 (2016).

[42] D. Kapner, Tests of the Gravitational Inverse-Square Law below the Dark-Energy Length Scale, *Physical Review Letters* **98**, 10.1103/PhysRevLett.98.021101 (2007).

[43] C. D. Hoyle, D. J. Kapner, B. R. Heckel, E. G. Adelberger, J. H. Gundlach, U. Schmidt, and H. E. Swanson, Submillimeter tests of the gravitational inverse-square law, *Physical Review D* **70**, 042004 (2004).

[44] S. Schreppler, N. Spethmann, N. Brahms, T. Botter, M. Barrios, and D. M. Stamper-Kurn, Optically measuring force near the standard quantum limit, *Science* **344**, 1486 (2014).

[45] I. Pikovski, M. R. Vanner, M. Aspelmeyer, M. S. Kim, and C. Brukner, Probing Planck-scale physics with quantum optics, *Nature Physics* , 393 (2012).

[46] A. Belenchia, R. M. Wald, F. Giacomini, E. Castro-Ruiz, v. Brukner, and M. Aspelmeyer, Quantum superposition of massive objects and the quantization of gravity, *Physical Review D* **98**, 126009 (2018).

[47] N. Ismail, C. C. Kores, D. Geskus, and M. Pollnau, Fabry-pérot resonator: spectral line shapes, generic and related airy distributions, linewidths, finesSES, and performance at low or frequency-dependent reflectivity, *Optics express* **24**, 16366 (2016).

[48] G. Cesini, G. Guattari, G. Lucarini, and C. Palma, Response of fabry-perot interferometers to amplitude-modulated light beams, *Optica Acta: International Journal of Optics* **24**, 1217 (1977).

[49] H. Carstens, N. Lilienfein, S. Holzberger, C. Jocher, T. Eidam, J. Limpert, A. Tünnermann, J. Weitenberg, D. C. Yost, A. Alghamdi, *et al.*, Megawatt-scale average-power ultrashort pulses in an enhancement cavity, *Optics letters* **39**, 2595 (2014).

[50] E. Sistrunk, D. A. Alessi, A. Bayramian, K. Chesnut, A. Erlandson, T. C. Galvin, D. Gibson, H. Nguyen, B. Reagan, K. Schaffers, C. W. Siders, T. Spinka, and C. Haefner, Laser Technology Development for High Peak Power Lasers Achieving Kilowatt Average Power and Beyond, in *Short-pulse High-energy Lasers and Ultrafast Optical Technologies*, Vol. 11034,

edited by P. Bakule and C. L. Haefner, International Society for Optics and Photonics (SPIE, 2019) pp. 1 – 8.

- [51] O. Schwartz, J. J. Axelrod, D. R. Tuthill, P. Haslinger, C. Ophus, R. M. Glaeser, and H. Müller, Near-concentric Fabry-Perot cavity for continuous-wave laser control of electron waves, *Optics Express* **25**, 14453 (2017).
- [52] E. Cartlidge, Physicists are planning to build lasers so powerful they could rip apart empty space, *Science | AAAS* (2018).
- [53] <https://www.ipgphotonics.com/de/products/lasers/high-power-cw-fiber-lasers>.
- [54] M. W. Krasny, A. Petrenko, and W. Płaczek, High-luminosity Large Hadron Collider with laser-cooled isoscalar ion beams, *Progress in Particle and Nuclear Physics* **114**, 103792 (2020).
- [55] V. N. Litvinenko, Coherent Electron Cooling, Brookhaven National Lab update on status of experimental demonstration (2017).
- [56] F. Marquardt and S. M. Girvin, Optomechanics, *Physics* **2** (2009), publisher: American Physical Society.
- [57] F. Marquardt and S. M. Girvin, Trend: optomechanics, *Physics* **2**, 40 (2009).
- [58] M. Metcalfe, Applications of cavity optomechanics, *Applied Physics Reviews* **1**, 031105 (2014).
- [59] J. Millen, T. S. Monteiro, R. Pettit, and A. N. Vamivakas, Optomechanics with levitated particles, *Reports on Progress in Physics* **83**, 026401 (2020).
- [60] O. Arcizet, P.-F. Cohadon, T. Briant, M. Pinard, A. Heidmann, J.-M. Mackowski, C. Michel, L. Pinard, O. Français, and L. Rousseau, High-sensitivity optical monitoring of a micromechanical resonator with a quantum-limited optomechanical sensor, *Physical review letters* **97**, 133601 (2006).
- [61] G. Ranjit, M. Cunningham, K. Casey, and A. A. Geraci, Zeptonewton force sensing with nanospheres in an optical lattice, *Physical Review A* **93**, 053801 (2016).
- [62] F. Schneiter, S. Qvarfort, A. Serafini, A. Xuereb, D. Braun, D. Rätzel, and D. E. Bruschi, Optimal estimation with quantum optomechanical systems in the nonlinear regime, *Phys. Rev. A* **101**, 033834 (2020).
- [63] S. Qvarfort, A. D. K. Plato, D. E. Bruschi, F. Schneiter, D. Braun, A. Serafini, and D. Rätzel, Optimal estimation of time-dependent gravitational fields with quantum optomechanical systems (2020), arXiv:2008.06507 [quant-ph].

[64] M. Maggiore, *Gravitational waves: Volume 1: Theory and experiments*, Vol. 1 (Oxford university press, 2008).

[65] D. Rätzel, F. Schneiter, D. Braun, T. Bravo, R. Howl, M. P. E. Lock, and Ivette Fuentes, Frequency spectrum of an optical resonator in a curved spacetime, *New Journal of Physics* **20**, 053046 (2018).

[66] A. A. Clerk, M. H. Devoret, S. M. Girvin, F. Marquardt, and R. J. Schoelkopf, Introduction to quantum noise, measurement, and amplification, *Reviews of Modern Physics* **82**, 1155 (2010).

[67] S. Singh, L. A. D. Lorenzo, I. Pikovski, and K. C. Schwab, Detecting continuous gravitational waves with superfluid<sup>4</sup>He, *New Journal of Physics* **19**, 073023 (2017).

[68] N. Matsumoto, S. B. Cataño-Lopez, M. Sugawara, S. Suzuki, N. Abe, K. Komori, Y. Michimura, Y. Aso, and K. Edamatsu, Demonstration of displacement sensing of a mg-scale pendulum for mm-and mg-scale gravity measurements, *Physical review letters* **122**, 071101 (2019).

[69] C. M. Caves, K. S. Thorne, R. W. P. Drever, V. D. Sandberg, and M. Zimmermann, On the measurement of a weak classical force coupled to a quantum-mechanical oscillator. I. Issues of principle, *Reviews of Modern Physics* **52**, 341 (1980).

[70] V. B. Braginsky, Y. I. Vorontsov, and K. S. Thorne, Quantum Nondemolition Measurements, *Science* **209**, 547 (1980).

[71] C. F. Ockeloen-Korppi, E. Damskägg, J.-M. Pirkkalainen, T. T. Heikkilä, F. Massel, and M. A. Sillanpää, Low-noise amplification and frequency conversion with a multiport microwave optomechanical device, *Phys. Rev. X* **6**, 041024 (2016).

[72] C. F. Ockeloen-Korppi, E. Damskägg, J.-M. Pirkkalainen, T. T. Heikkilä, F. Massel, and M. A. Sillanpää, Noiseless quantum measurement and squeezing of microwave fields utilizing mechanical vibrations, *Phys. Rev. Lett.* **118**, 103601 (2017).

[73] L. Zhong, E. P. Menzel, R. D. Candia, P. Eder, M. Ihmig, A. Baust, M. Haeberlein, E. Hoffmann, K. Inomata, T. Yamamoto, Y. Nakamura, E. Solano, F. Deppe, A. Marx, and R. Gross, Squeezing with a flux-driven Josephson parametric amplifier, *New Journal of Physics* **15**, 125013 (2013).

[74] L. D. T’oth, N. R. Bernier, A. Nunnenkamp, A. K. Feofanov, and T. J. Kippenberg, A dissipative quantum reservoir for microwave light using a mechanical oscillator, *Nature Physics*

**13**, 787 (2017).

- [75] J. M. E. Fraïsse and D. Braun, Coherent averaging: Coherent averaging, *Ann. Phys. (Berlin)*, 1 (2015).
- [76] D. Braun and S. Popescu, Coherently enhanced measurements in classical mechanics, *Quantum Measurements and Quantum Metrology* **2** (2014).
- [77] D. Hartwig, J. Petermann, and R. Schnabel, Mechanical parametric feedback-cooling for pendulum-based gravity experiments, *arXiv:2012.12158* (2020).
- [78] e. a. Aasi, Enhanced sensitivity of the LIGO gravitational wave detector by using squeezed states of light, *Nature Photonics* **7**, 613 (2013).
- [79] H. Vahlbruch, M. Mehmet, K. Danzmann, and R. Schnabel, Detection of 15 dB Squeezed States of Light and their Application for the Absolute Calibration of Photoelectric Quantum Efficiency, *Physical Review Letters* **117**, 110801 (2016).
- [80] G. Keller, V. D'Auria, N. Treps, T. Coudreau, J. Laurat, and C. Fabre, *Optics Express* **16**, 9351 (2008).
- [81] Y. I. Alexahin, On the Landau Damping and Decoherence of Transverse Dipole Oscillations in Colliding Beams (1996), number: CERN-SL-96-064-AP Pages: 43-74 Volume: 59.
- [82] X. Buffat, G. Papotti, W. Herr, R. Calaga, T. Pieloni, R. Giachino, and S. White, Coherent beam-beam mode in the LHC (2014), contribution to the ICFA Mini-Workshop on Beam-Beam Effects in Hadron Colliders, CERN, Geneva, Switzerland, 18-22 Mar 2013 pp.227-230, *arXiv:1410.5695*.
- [83] Y. Alexahin, H. Grote, W. Herr, and M. Zorzano, COHERENT BEAM-BEAM EFFECTS IN THE LHC, *CERN-LHC-PROJECT-REPORT-469* Proceedings, 18th International Conference on High-Energy Accelerators, 5 (2001).
- [84] M. P. Zorzano and F. Zimmermann, Coherent Beam-Beam Oscillations at the LHC., *LHC Project Report* 314 , 19 (1999).
- [85] K. Yokoya and H. Koiso, TUNE SHIFT OF COHERENT BEAM-BEAM OSCILLATIONS, *Part. Accel.* **27**, [427]/181 (1990).
- [86] J. P. Schiffer and P. Kienle, Could there be an ordered condensed state in beams of fully stripped heavy ions?, *Zeitschrift für Physik A Atoms and Nuclei* **321**, 181 (1985).
- [87] T. Schätz, U. Schramm, and D. Habs, Crystalline ion beams, *Nature* **412**, 717 (2001), number: 6848 Publisher: Nature Publishing Group.

[88] J. Wei and A. M. Sessler, Crystalline beams, in *18th Advanced ICFA Beam Dynamics Workshop on Quantum Aspects of Beam Physics* (AIP, 2003) p. 176.

[89] M. Tanabe, T. Ishikawa, M. Nakao, H. Souda, M. Ikegami, T. Shirai, H. Tongu, and A. Noda, Longitudinal and Transverse Coupling of the Beam Temperature Caused by the Laser Cooling of  $^{24}\text{Mg}^+$ , *Applied Physics Express* **1**, 028001 (2008).

[90] U. Schramm, T. Schätz, and D. Habs, Bunched Crystalline Ion Beams, *Physical Review Letters* **87**, 184801 (2001).

[91] U. Schramm, T. Schätz, M. Bussmann, and D. Habs, Cooling and heating of crystalline ion beams, *Journal of Physics B: Atomic, Molecular and Optical Physics* **36**, 561 (2003).

[92] U. Schramm, T. Schätz, and D. Habs, Bunched crystalline ion beams, *Phys. Rev. Lett.* **87**, 184801 (2001).

[93] K. Brown and T. Roser, Towards storage rings as quantum computers, *Physical Review Accelerators and Beams* **23**, 054701 (2020).

[94] A. M. Sessler, The cooling of particle beams, in *AIP Conference Proceedings*, Vol. 356 (Austin, Texas (USA), 1996) pp. 391–407.

[95] M. Steck, Beam cooling, Talk at CAS Warsaw (2015), [indico.cern.ch/event/361988/contributions/1775715/attachments/1157463/1697398/beamcooling-steck-cas2015.pdf](https://indico.cern.ch/event/361988/contributions/1775715/attachments/1157463/1697398/beamcooling-steck-cas2015.pdf).

[96] V. N. Litvinenko and Y. S. Derbenev, Coherent Electron Cooling, *Physical Review Letters* **102**, 114801 (2009).

[97] V. N. Litvinenko, G. Wang, D. Kayran, Y. Jing, J. Ma, and I. Pinayev, Plasma-Cascade micro-bunching Amplifier and Coherent electron Cooling of a Hadron Beams, arXiv:1802.08677 [physics] (2018).

[98] J. S. Hangst, M. Kristensen, J. S. Nielsen, O. Poulsen, J. P. Schiffer, and P. Shi, Laser cooling of a stored ion beam to 1 mK, *Physical Review Letters* **67**, 1238 (1991).

[99] S. Schröder, R. Klein, N. Boos, M. Gerhard, R. Grieser, G. Huber, A. Karafillidis, M. Krieg, N. Schmidt, T. Kühl, R. Neumann, V. Balykin, M. Grieser, D. Habs, E. Jaeschke, D. Krämer, M. Kristensen, M. Music, W. Petrich, D. Schwalm, P. Sigray, M. Steck, B. Wanner, and A. Wolf, First laser cooling of relativistic ions in a storage ring, *Physical Review Letters* **64**, 2901 (1990).

- [100] H.-J. Miesner, Efficient, Indirect Transverse Laser Cooling of a Fast Stored Ion Beam, *Physical Review Letters* **77**, 623 (1996).
- [101] P. C. Vaidya, The gravitational field of a radiating star, in *Proceedings of the Indian Academy of Sciences-Section A*, Vol. 33 (Springer, 1951) p. 264.